HHS Public Access

Author manuscript

Adv Exp Med Biol. Author manuscript; available in PMC 2024 July 15.

Published in final edited form as:

Adv Exp Med Biol. 2021 ; 1349: 195–223. doi:10.1007/978-981-16-4254-8_10.

Glial Chloride Channels in the Function of the Nervous System Across Species

Jesus Fernandez-Abascal,

Bianca Graziano,

Nicole Encalada,

Laura Bianchi

Department Physiology and Biophysics, University of Miami, Miller School of Medicine, Miami, FL, USA

Abstract

In the nervous system, the concentration of Cl^- in neurons that express GABA receptors plays a key role in establishing whether these neurons are excitatory, mostly during early development, or inhibitory. Thus, much attention has been dedicated to understanding how neurons regulate their intracellular Cl^- concentration. However, regulation of the extracellular Cl^- concentration by other cells of the nervous system, including glia and microglia, is as important because it ultimately affects the Cl^- equilibrium potential across the neuronal plasma membrane. Moreover, Cl^- ions are transported in and out of the cell, via either passive or active transporter systems, as counter ions for K^+ whose concentration in the extracellular environment of the nervous system is tightly regulated because it directly affects neuronal excitability. In this book chapter, we report on the Cl^- channel types expressed in the various types of glial cells focusing on the role they play in the function of the nervous system in health and disease. Furthermore, we describe the types of stimuli that these channels are activated by, the other solutes that they may transport, and the involvement of these channels in processes such as pH regulation and Regulatory Volume Decrease (RVD). The picture that emerges is one of the glial cells expressing a variety of Cl^- channels, encoded by members of different gene families, involved both in short- and long-term regulation of the nervous system function. Finally, we report data on invertebrate model organisms, such as *C. elegans* and Drosophila, that are revealing important and previously unsuspected functions of some of these channels in the context of living and behaving animals.

Keywords

Glial chloride channels; Channelopathies; Neuron; glia interaction; Nervous system development; ClC-2; LRRC8; SWELL1; VRAC; Bestrophins; Maxi chloride channels; Pannexins

✉L. Bianchi, lbianchi@med.miami.edu.

10.1 ClC-2

10.1.1 Structure and Function

Encoded by the *CLCN2* gene, ClC-2 is a plasma membrane voltage-gated chloride (Cl^-) channel that is expressed in most mammalian tissues [1]. In brain cells, ClC-2 protein and currents are present in neurons and glial cells such as astrocytes and oligodendrocytes [2–5]. This channel is a member of the ClC family of voltage-gated Cl^- channels, characterized by a double-barreled structure with two independent pores, one in each subunit, and two intracellular conserved cystathionineβ-synthase (CBS) domains in the C-terminus, which are involved in gating regulation (Fig. 10.1a, b) [9, 10]. ClC-2 is an inward rectifying channel that remains closed at positive potentials and is activated by hyperpolarizing voltages (Fig. 10.1c) [11]. However, channels formed by one ClC-2 and one ClC-1 (or ClC-0) subunit are also partially open at positive potentials (Fig. 10.1c, d) [12, 13].

ClC-2 gating is also regulated by intracellular and extracellular ions. Intracellular Cl^- regulates ClC-2 gating by pore occupancy, promoting conformational changes to the gate that allow for the opening of the channel [14]. Conversely, extracellular protons (H^+) open the channel at low concentrations but block it at high concentrations [15, 16]. Concerning the role of Cl^- and H^+ on ClC-2 channel gating, Sanchez-Rodriguez and colleagues proposed that while intracellular Cl^- is responsible for the opening of ClC-2, extracellular H^+ stabilizes the open state of the channel (Sanchez-Rodriguez et al. [17]. Cell swelling is another mechanism by which ClC-2 is activated; yet, according to a recent review, this channel does not seem to be a major contributor to cell volume regulation [18, 19].

10.1.2 ClC-2 in the Vertebrate Brain

As mentioned earlier, ClC-2 is expressed both in neurons and in glia. In neurons, ClC-2 has been proposed to regulate neuronal excitability likely via regulation of Cl^- concentration inside and outside the cell, which consequently affects the neuronal membrane potential. Rinke and colleagues demonstrated that in mouse CA1 pyramidal cells, ClC-2 participates in Cl^- efflux [11]. One year later, Ratte and Prescott [20] reported opposite results for rat CA1 pyramidal cells and stated that ClC-2 participates in Cl^- influx, resulting in reduced neuronal excitability. This conflicting finding might be the result of differences in experimental conditions since in the first study neurons were loaded with high Cl^- concentrations, while in the second study physiological solutions were used.

Despite the proposed role of neuronal ClC-2 in regulating excitability, a link between ClC-2 and excitability disorders such as epilepsy has not been firmly established. ClC-2 was proposed to participate in controlling GABA neurons' excitability; however, the screening of epileptic patients for mutations in *CLCN2* provided inconclusive results. This suggests that mutations in *CLCN2* might increase susceptibility to epilepsy in individuals with other underlying conditions or with mutations in other genes [21]. *CLCN2* loss-of-function mutations have also been linked to cerebellar ataxia and minor cognitive defects that could be attributed to the ClC-2 role in either glia or neurons [22].

In glia, the function of ClC-2 is strongly supported by a correlation between mutations in the *CLCN2* gene and either phenotype in animal models or pathology in humans. In humans,

mutations in *CLCN2* have been linked to a type of leukodystrophy called megalencephalic leukoencephalopathy with subcortical cysts (MLC) [23–25]. In this disease, the brain is enlarged showing signs of edema and the white matter is characterized by atrophy, vacuoles, and cysts that worsen with time. In these patients, mutations in ClC-2 cause mislocalization or dysfunction of the channel, both of which have been proposed to result in white matter pathology [6]. In an analytical study of patients with this disease, Depienne and colleagues observed that myelin vacuolization is present in both the brain and the spinal cord [23]. This neurological phenotype supports the role of ClC-2 in the function and survival of glia, in particular of oligodendrocytes throughout the central nervous system, but not in the peripheral nervous system. Similarly, in a mouse model in which the corresponding rodent gene has been knocked out, there is widespread vacuolation that progresses with age. Interestingly, as seen in humans, vacuolation is limited to the white matter and is not seen in the gray matter, again underscoring ClC-2 function in glia [6].

Remarkably, megalencephalic leukoencephalopathy with subcortical cysts can be caused by mutations in other two genes: *MLC1* [8], encoding a protein predicted to have eight transmembrane domains and *GLIALCAM* [7, 26], which encodes the adhesion molecule GlialCAM of the immunoglobulin superfamily, highly expressed in glial cells. Based, on the similarity of the pathological manifestations and expression pattern of these three proteins, ClC-2, GLIALCAM, and MLC1 have been proposed to interact and regulate each other (Fig. 10.1e). Evidence that supports this idea are: (1) all three proteins colocalize to the endfeet contacting blood vessels and at astrocyte–astrocyte contacts [6, 7], (2) GlialCAM directs ClC-2 and MLC1 to cell–cell contacts of heterologously transfected cells, and (3) ClC-2 localization and function are controlled by the interaction with both GlialCAM and MLC1. Indeed, knock-out of either GlialCAM or MLC1 in mice results in impaired localization of ClC-2 in astrocytes and oligodendrocytes and in altered inward current rectification. In particular, in GlialCAM$^{-/-}$ or MLC1$^{-/-}$, ClC-2 is localized in the soma instead of the cellular processes [8]. Similarly in zebrafish, two ClC-2 orthologs, clc-2a and clc-2b, are expressed in astrocyte-like cells and interact with the GlialCAM paralog, glialcama, suggesting that targeting and stabilization of ClC-2 in the glial plasma membrane by GlialCAM-like proteins might be an evolutionary conserved mechanism [27].

Based on the mice knock-out phenotype and the neuroanatomical and neurological features observed in subjects with mutations in *CLCN2* and ClC-2 regulatory genes GlialCAM or MLC1, a function for ClC-2 has been suggested. It has been proposed that ClC-2 might function as a pathway for the release and reuptake of Cl^- from the cell that follows K^+ movement during high neuronal activity [4]. Indeed, the movement of ions across the plasma membrane during action potential discharge is normally followed by osmotically driven shifts in water. Thus, anything that interferes with the compensatory movement of Cl^- and water is expected to cause brain edema and leukodystrophy, both of which are observed in *CLCN2* knock-out mice and in patients with mutations in this gene [23].

This function of ClC-2 might be particularly important in brain regions with GABAergic synapses, where regulation of Cl^- concentration plays a key role in maintaining efficient GABAergic transmission. Indeed, Sik and colleagues, using immunostaining and electron microscopy, found that ClC-2 is expressed in CA1 pyramidal neurons, especially in the

plasma membrane of dendrites closely associated with synaptic active zones [28]. ClC-2 was also present in the end feet of astrocytes ensheathing capillaries and blood vessels, and in the neuropil of the stratum pyramidale, in close proximity to GABAergic neurons. In addition, the level of expression of ClC-2 was polarized in astrocytes and it was layer-specific. These findings lead the authors to propose a role for glial ClC-2 in the reuptake of Cl^- and redistribution of this ion over the different brain areas, suggesting that ClC-2 actively participates in K^+ siphoning, the phenomenon by which K^+ is removed from the extracellular environment and dumped into the blood stream during high neuronal activity.

Interestingly, ClC-2 currents are smaller in in situ astrocytes of P19 versus P60 mice and lower in situ hybridization staining for ClC-2 is also observed in neonatal versus adult hippocampus [29, 30]. These observations correlate with the GABA switch during development, suggesting that ClC-2 participates with KCC transporters in regulating Cl^- concentration in the brain. They also correlate with the progressive white matter pathology seen in individuals with mutations in *CLCN2* gene and in ClC-2 knockout mice models.

Makara and colleagues also found downregulation of ClC-2 currents in reactive astrocytes around a stab lesion, suggesting, in this case, that dysregulation of the ClC-2 currents might contribute to neuronal demise [29]. In contrast, Zhao and colleagues more recently found that the injection of Cl^- channel blocker DIDS protects against white matter damage in a model of chronic cerebral ischemia–hypoxia in the rat via reduction of ClC-2 protein levels [31]. Similarly, in a diabetes rat model, high glucose concentrations were found to increase the ClC-2 activity and to promote white matter damage, which is ameliorated by the administration of DIDS [32]. These contrasting results might derive in the last two studies from the use of DIDS, a nonspecific Cl^- channel blocker.

The function of ClC-2 in controlling ionic homeostasis in the extracellular environment was suggested by Bosl and colleagues in other two organs, the eye and the testis [33]. Studies in these organs were prompted by the fact that ClC-2 knockout mice are blind and sterile. Careful analysis of the retina and testes extracted from ClC-2 knockout mice demonstrated that the cause of blindness and sterility was massive degeneration of the photoreceptors and the spermatocytes, respectively. Interestingly though, ClC-2 is not expressed in these cells. The investigators found that ClC-2 is expressed in supporting epithelial cells that are responsible in these two organs for creating an isolated microenvironment where photoreceptors and spermatocytes develop. These observations lead Bosl and colleagues to speculate that ClC-2 might be required to regulate ionic homeostasis in this microenvironment between support cells and principal cells [33]. This idea is in line with what is observed in the nervous system where ClC-2 is expressed in glia that are tasked with controlling ionic homeostasis in the microenvironment surrounding neurons.

Changes in ClC-2 expression levels near GABAergic synapses during the lifespan of the mouse clearly underscores that the function of ClC-2 might be more critical during certain life stages [11]. This is also evident when studying the pathology of knock-out models of ClC-2 regulatory genes MLC1 and GlialCAM. For example, using histological and electron microscopy approaches, Dubey and colleagues showed that vacuolization in the white matter

in *Mlc1*-null mice begins at 3 months of age, suggesting that ClC-2 function is more critical in adults than in juvenile mice [34]. In a *Glialcam*-null mouse model, the vacuolization begins earlier (3 weeks of age), but this could be due to the fact that GlialCAM may have other functions that are independent of MLC1 and ClC-2 [35]. Importantly, both in patients and in megalencephalic leukoencephalopathy mice models, myelination appears normal [34, 35]. These findings support that oligodendrocytes lacking ClC-2 can still efficiently insulate axons during development.

10.1.3 Insights into the Function of Glial ClC Channels from Studies in Invertebrates

A study in the fruit fly Drosophila melanogaster suggests a role for ClC-2 type channels in early nervous system development that might explain the cerebellar ataxia and cognitive deficits found in some patients with null mutations in *CLCN2* [36]. Indeed, Plazaola and colleagues generated loss-of-function mutants for ClC-2 fly homolog ClC-a and observed that these flies have a smaller brain and defective photoreceptor guidance [37]. Using confocal microscopy and genetic approaches, they found that ClC-a is required in the niche of glial cells for the development of neuroepithelial cells and neuroblast as well as for the maturation of neurons outside the niche (Fig. 10.2a, b). The authors also found that ClC-a is important for the formation of a specific tissue called the medulla glia which is responsible for photoreceptor guidance. Plazaola-Sasieta and colleagues proposed two possible explanations for the phenotypes observed in the ClC-a knockout fly: (1) impaired secretion of glial factors, including tropic factors and guidance cues, due to imbalance in Cl^- homeostasis and (2) impaired proliferative capacity of stem cells due to alterations in pH regulation. ClC-2 type channels have been proposed to function in mediating Cl^- movement across the membrane in exchange for bicarbonate, the major pH buffering system in our body [39].

Interestingly, our lab showed that CLH-1, a *Caenorhabditis elegans* Cl^- channel that shares 37% identity with ClC-2, is expressed in glia and is permeable to bicarbonate (HCO_3^-) [38]. Using the pH sensor phluorin, we showed that *clh-1* knockout animals have impaired HCO_3^--dependent pH buffering in amphid sheath glia, which can be restored by the rescue of CLH-1 in these cells (Fig. 10.2c–f). By electrophysiological analysis, we also showed that CLH-1 is an inward rectifier channel activated by extracellular acidification. We thus proposed that CLH-1 might be activated by extracellular acidification and contribute to pH buffering of the extracellular environment via HCO_3^- permeation. Our study suggests that pH buffering mediated by ClC-2 type channels could be mediated via direct permeation of HCO_3^- and/or via regulation of bicarbonate transporters by exchange of Cl^- for HCO_3^-, as mentioned earlier.

A more recent study by Park et al. [40] reports a role for CLH-1 in the regulation of neuronal response to salt stimuli. Using Cl^- and Ca^{2+} sensors, Park and colleagues showed in vivo that the response of the ASER neuron to Na^+ is regulated by CLH-1. Using cell-specific promoters, they demonstrated that the role of CLH-1 in salt sensing is mediated by the expression of the channel in this sensory neuron and not in amphid sheath glia. This study suggests that the function of CLH-1 in neurons and glia might be distinct and may be responsible for regulating different aspects of the function of the nervous system.

10.2 Acid and Swelling-Activated Cl^- Channels (LRRC8 or SWELL1)

During neuronal activity, there are rapid changes in pH and cell volume, the last ones caused by the movement of K^+ and Cl^- ions, which need to be precisely corrected to ensure the functioning of the nervous system. To regulate cell volume and pH, astrocytes and microglia (among other cell types) are thought to use volume-sensitive anion channels (VRAC) [41], also known as volume-sensitive organic anion channels (VSOAC) and volume-activated chloride channels (VACC).

More specifically, VRAC is activated by cell swelling and plays a key role in regulatory volume decrease (RVD). RVD is a process by which all cells activate membrane transporters and channels to reduce their volume following events that cause cell swelling (Fig. 10.3a). VRAC, by mediating the efflux of Cl^- and organic osmolytes such as glutamate, taurine, and possibly ATP, coupled to efflux of K^+ via K^+ channels, bring cell volume down to control levels [44, 45]. Importantly, as we discuss below, in the nervous system, the release of glutamate, taurine, and ATP by VRAC, is thought to participate in gliotransmission.

Across cell types, VRAC has been implicated in processes such as cell cycle progression and migration, which are characterized by an increase in cell volume, and in apoptosis, which is on the contrary characterized by volume decrease [46]. In this case, VRAC is activated under isovolumetric conditions by mitochondrial-mediated apoptosis inducers (possibly src-like tyrosine kinase p56LcK) that are triggered by reactive oxygen species (ROS) production [47, 48].

The first evidence of Cl^- channel-mediated volume regulation in glial cells was reported by Pasantes-Morales and colleagues, who showed that exposure to hypoosmotic solutions caused the release of taurine from cultured rat astrocytes, which was blocked by Cl^- channels inhibitors DIDS, dipyramidole, and niflumic acid [49, 50]. A few years later, Bakhramov and colleagues described a weak outwardly rectifying Cl^- current in cultured astrocytoma activated by exposure to hypotonic solutions and suggested that this current was mediated by VRAC [51]. The current was activated slowly with a time course of 1–2 min, had a half-maximum inactivation of +50 mV, and was blocked by Cl^- channel blockers DIDS, SITS, and NPPB. Following these initial reports, many other investigators described Cl^- currents resembling VRAC in glial cells. For example, in a study using rat cortical astrocytes, Parkerson and colleagues proposed that VRAC was the major contributor to RVD in these cells [52]. This was further confirmed 2 years later by Abdullaev and colleagues who showed that both the release of excitatory amino acids (EAA) and Cl^- currents were specifically inhibited by VRAC blockers but not by other Cl^- channels/transporters blockers [53].

How does VRAC become activated by volume increase? A few mechanisms have been suggested. For example, using immunoblotting, confocal microscopy, and patch-clamp experiments, Ando-Akatsuka and colleagues proposed that under isovolumetric conditions VRAC is inhibited by interaction with ATP-binding cassette transporter (ABCF2). When the cell is challenged by a hypotonic solution, its volume increases which cause the interaction between ATP-binding cassette transporter (ABCF2) and the channel to be disrupted. The

disruption of this molecular interaction is due to the association of ABCF2 with α-actinin-4 (ACTN4) [54]. In another study, using patch-clamp and imaging techniques, Murana and colleagues proposed that activation of VRAC in mouse hippocampal microglia is caused by membrane stretch and is subsequently amplified by the raise of intracellular Ca^{2+} which is in turn mediated by activation P2Y purinergic receptors [44]. Importantly, the investigators proposed that P2Y purinergic receptors are themselves activated by ATP released by VRAC, suggesting that VRAC channels can be potentiated via a positive feedback mechanism. Interestingly, in another study VRAC amplification by ATP was shown to be mediated by two different Ca^{2+}-sensitive signaling cascades involving both PKC and CaMK II [55]. Finally, in a recent study, Konig and colleagues used Förster resonance energy transfer (FRET) to monitor the opening of VRAC channels and determined that changes in the intracellular ionic strength are not needed for channel activation. Rather, channel activation is dependent on the DAG-Protein Kinase D pathway [56]. To conclude, there are a few different hypotheses on the mechanism underlying VRAC activation, suggesting either that the mechanism is cell specific or that it is not fully understood. The recent cloning of the gene underlying VRAC and the resolution of the protein structure should help in solving this debate.

In 2014, the long-standing controversy on the molecular identity of VRAC came to an end when two groups independently reported that the Leucine-rich repeat containing 8A (LRRC8A), renamed by one of the two groups SWELL1, encoded VRAC [57, 58]. Using a clever method developed by Galietta and colleagues [59], which exploits the quenching properties of I^- on YFP fluorescence, both groups performed large siRNA screens and demonstrated that siRNA of LRRC8A in HEK cells resulted in knock-down of VRAC. LRRC8A is one of five related genes encoding homologous subunits that span the plasma membrane four times leaving N and C termini in the cytosol (Fig. 10.3b, c), a structure that resembles connexins, pannexins, and innexins with which LRRC8A share some degree of homology [18]. The name of the family derives from the intracellular LRR domain (LRRD) which contains up to 15–16 leucine repeats (Fig. 10.3b). Interestingly, while LRRC8A expresses on its own in heterologous expression systems, it still needs one of the other subunits for full expression of the current (Fig. 10.3d, e) [43, 58]. Moreover, functional expression of all the other subunits (LRRC8B-E) requires LRRC8A [58]. These results suggest that LRRC8B-E might function more as regulatory subunits.

The function of the LRRC8B-E subunits as regulators of channel properties is reflected in the fact that channel permeability is altered when LRRC8B-E subunits are removed from the channel complexes. For example, Schober and colleagues, using RNAi to knockdown individual subunits of the channel, studied the release of [^{3}H]taurine (inhibitory) and D-[^{14}C]aspartate (excitatory). They showed that while LRRC8A is an essential channel subunit, LRRC8B does not seem to participate in channel selectivity, and LRRC8D is a major contributing factor in conferring selectivity to [^{3}H]taurine [45]. In the same study, the investigators also showed that the combined knockdown of LRRC8C and LRRC8E inhibited the release of D-[^{14}C]aspartate but not [^{3}H]taurine. Based upon these results, the authors concluded that different regions of the nervous system, depending on the expression patterns of the LRRC8 subunits, might release different sets of gliotransmitters, including excitatory glutamate/aspartate and inhibitory taurine/glycine. The authors also propose that the regional

specific release of these gliotransmitters might be altered in pathological conditions such as trauma, stroke, hyponatremia, and epilepsy all of which are characterized by cell swelling.

The excitatory/inhibitory amino acids that are released by glial-expressed VRAC are thought to mediate regulation of neuronal function/survival, especially during pathological conditions such as ischemia and trauma in which there are changes in cell volume. For example, Liu and colleagues showed in cultured rat astrocytes that cell swelling and ischemic stimuli cause the release of glutamate, which is at least in part inhibited by the VRAC inhibitor phloretin [60]. VRAC activation and release of glutamate can occur also under isovolumetric conditions. Indeed, Liu and colleagues showed in rat co-cultures that activation by bradykinin of astrocytic VRAC leads to an increase of intracellular Ca^{2+} in neurons which is mediated by NMDA receptors. These data indicate that VRAC mediates the release of glutamate from astrocytes which in turn mediates glia/neuron functional interaction [61].

Although VRAC has been shown to release excitatory glutamate/aspartate and inhibitory taurine/glycine, its role in gliotransmission is still controversial. Nevertheless, new insights into the modulation of neuronal function by glutamate released from astrocytes via VRAC have been published in a recent study by Yang and colleagues [62]. These authors generated a mouse model in which the VRAC subunit LRRC8A (SWELL1) had been knocked out specifically in astrocytes. Using a combination of electrophysiology and the “sniffer patch” technique to monitor both neuronal activity and release of glutamate, they showed that, upon osmotic challenges, glutamatergic synaptic transmission and synaptic plasticity in the hippocampus were impaired in these knock-out mice (Fig. 10.4). Furthermore, they showed that there is tonic glutamate release from astrocytes and this is mostly mediated by VRAC. Reduced tonic release of glutamate in the knock-out mice results in fewer action potentials in neurons, suggesting that it serves a function in regulating neuronal activity. Importantly, these cellular phenotypes are reflected in behavioral phenotypes. Indeed, LRRC8A knock-out mice showed impaired cognitive abilities including deficits in learning and memory, while locomotion and anxiety levels remained unaffected. These new data support a physiological role of astrocytic VRAC channels in modulating neuronal excitability by maintaining a tonic concentration of glutamate in the extracellular environment, a role that had been already suggested by previous studies using VRAC blockers [63, 64].

The release of glutamate by astrocytes mediated by VRAC can become toxic in pathological conditions. For example, during ischemia, hypoxic conditions induce swelling and consequently the excessive release of glutamate by astrocytes that in turn causes persistent elevation of intracellular Ca^{2+} concentration in neurons, ultimately causing cell death [65]. VRAC blockers such as tamoxifen and DCPIB were shown to reduce glutamate-induced neuronal death, suggesting that this channel mediates, at least in part, the persistent release of glutamate under these conditions [66]. Importantly, the above-mentioned LRRC8A (SWELL1) astrocytic knock-out mouse model confirms that VRAC is indeed responsible for at least some of the neuronal damage in stroke. Yang and colleagues used temporal middle cerebral artery occlusion to induce stroke and showed that the infarct volume was smaller in LRRC8A knock-out mice when compared to control, which was also reflected in a better neurological score in these mice [62].

Cell swelling and glutamate release occur also during epileptic seizures. However, the role of VRAC in releasing glutamate in epilepsy is currently controversial. In rat models of epilepsy, Tian and colleagues using in vivo two-photon imaging, electrophysiology, and HPLC showed that seizures can be induced or amplified by glutamate released from astrocytes [67]. Interestingly, under these conditions, glutamate is co-released with taurine suggesting that it might be via VRAC. However, more recently, Woo and colleagues using channel blockers and siRNA showed that glutamate release from astrocytes is via the glutamate permeable two pore domains K^+ channel TREK-1, following activation of G-protein coupled receptors (fast release), and via Cl^- channel Bestrophin-1 (Best1) (slow release) [68]. Taken together these reports highlight that glutamate (and other transmitters) might be released via VRAC but also via other types of glial ion channels, all of which might contribute under different conditions to physiological and aberrant gliotransmission in the healthy and diseased brain.

While model organisms have been instrumental in deepening our understanding of the role of glial ClC Cl^- channels in the function of the nervous system, they have not been helpful for understanding VRAC. The reason is that there are no clear homologs of LRRC8 in *C. elegans* or *Drosophila melanogaster*, where the function of VRAC may be carried out by bestrophins. In the future, the analysis or other cell-specific LRRC8 knock-out mice should help elucidate the function of VRAC in other types of glial cells such as oligodendrocytes, Schwann cells, and microglia both under physiological and pathological conditions.

10.3 Acid-Sensitive Outwardly Rectifying (ASOR) Anion Channels

Strong acidification at pHs lower than 5.5 evokes outwardly rectifying chloride currents with electrophysiological features similar to those observed in VRAC and ClC channels. Several studies have shown currents with these properties in different cell types, including glia [69]. For example, using whole-cell electrophysiology, Lambert and Oberwinkler reported an outwardly rectifying current activated at low extracellular pH in HEK cells. They showed that this current is voltage- and extracellular Cl^--dependent, needs the binding of three or four protons to be activated, and it is blocked by DIDS and niflumic acid. In the same study, these investigators recorded currents with similar electrophysiological and pharmacological properties in primary mice hippocampal astrocytes [70]. These pH-sensitive currents not only resembled ClC type channels and VARC in terms of voltage dependence and kinetics, but they were also sensitive to the same inhibitors [70–72].

For this reason, ClC-3, ClC-7, and LRRC8A were postulated to underlie this Cl^- current activated by strong acidification in astrocytes [73, 74]. However, this molecular identity was never confirmed. For example, Auzanneau and colleagues used whole-cell patch-clamp and RT-PCR to show that the outwardly rectifying acid-activated chloride currents evoked in rat Sertoli cells were not mediated by the ClC channels [71]. In another study, the involvement of LRRC8A in mediating ASOR currents was also discarded by pharmacological and small-interfering RNA (siRNA) approaches. Indeed, classical VRAC inhibitors, as well as silencing of the LRRC8 isoforms using siRNA had no effect on the outwardly rectifying acid-evoked currents recorded in HeLa cells [75]. Similar observations were also reported in microglia BV-2 cell cultures by Kittl and colleagues, who demonstrated by patch-clamp

and fluorometric techniques that both ASOR and VRAC currents are activated in these cells under acidic conditions but with a different half maximal activation. So pH lower than 5 activates ASOR but inactivates VRAC. Moreover, the two Cl^- currents can be distinguished using pharmacological agents with only DIDS being equally effective in blocking both currents [76].

In two simultaneous studies recently published, the molecular basis of the ASOR channels was finally elucidated [77, 78]. Yang and colleagues used fluorescence to measure acid-induced Cl^- currents in HEK cells. The investigators then, knocked down by siRNA 2725 human proteins, predicted to have at least two transmembrane domains (Fig. 10.5a) and measured cellular fluorescence indicative of the amplitude of the Cl^- current. Using this method, the investigators identified the uncharacterized transmembrane protein 206 (TMEM206) as a possible candidate for the ASOR channel, as its knockdown caused reduction of acid-induced Cl^- currents. To test the involvement of TMEM206 in mediating ASOR currents, Yang and colleagues used a combination of CRISPR-cas9 to inactivate the gene and whole-cell patch clamp. They confirmed that indeed TMEM206 is required for acid activation of chloride currents in HEK cells [78]. Ullrich and colleagues used a similar fluorescent approach to perform a genome-wide screening with siRNA in HeLa cells and also concluded that TMEM206 underlies the ASOR current [77]. Importantly, both groups report that TMEM206 is highly expressed in CNS, especially in the cortex and hippocampus, and suggest a possible role of TMEM206 channels in acidotoxicity and ischemic brain injury [77–79]. No studies have been conducted yet to establish whether TMEM206 is expressed in neurons, glia, or both. However, previously published work suggests that TMEM206 might be expressed at least in astrocytes and microglia [70, 76].

Interestingly, both groups also report that TMEM206 is present in the genome of several other vertebrates including mouse, rat, chicken, frog, as well as zebrafish and conserves general functional features including activation by extracellular acidification and outward rectification (Fig. 10.5b). However, pH sensitivity and selectivity of TMEM206 and homologs appear to be more species specific. In other species such as the polychaete worm Capitella teleta and the sponge Amphimedon queenslandica, there are genes that have some degree of homology suggesting that TMEM206 may have appeared early in evolution. However, no clear homolog can be identified in *C. elegans* or Drosophila.

10.4 Maxi Chloride Channels

The maxi Cl^- channel (MAC) is a channel of high unitary current expressed in most human tissues, including the nervous system, where it has been observed in astrocytes and Schwann cells [80–83]. In addition to having a large conductance, MAC displays an ohmic current–voltage relationship, a strong selectivity for anions over cations ($PCl^-/PNa^+ > 8$), a sensitivity to Gd^{3+}, which blocks the channel, and voltage-dependent inactivation [81, 84]. The MAC channel is also inhibited by intracellular ATP via phosphorylation of tyrosine residues [85, 86]. Thus, the excision of a patch containing the MAC channel in a solution devoid of ATP induces its strongest activation [81, 86, 87]. In 2017 [88], Sabirov and colleagues using a combination of siRNA and electrophysiology discovered that the MAC channel is encoded by the *SLCO2A1* gene, a prostaglandin transporter (PGT) [88]. How

might a prostaglandin transporter function also as a large conductance Cl^- channel? Sabirov and colleagues suggested that SLCO2A1 functions in two modes: as a PGT in the resting state, most likely with phosphorylated tyrosine residues, and as a large conductance Cl^- channel in the activated state, presumably following dephosphorylation of tyrosine residues [88].

In glial cells, the first report of high unitary anion conductance was by Gray and colleagues, who used patch clamp to study endogenous currents of rat cultured Schwann cells. The investigators found a Cl^- channel with a conductance of ~450 pS, a linear current–voltage relationship, and inactivation kinetics at small positive and negative voltages [80]. Later, other groups reported the presence of currents with similar electrophysiological properties in cultured mouse and rat astrocytes [81–83]. The channel observed in these preparations is not only permeable to chloride and other anions, with a permeability sequence of $I^- > Br^- > Cl^- > F^-$, but also to organic molecules such as glutamate and ATP [60, 89]. Indeed, Liu and colleagues demonstrated that in mouse astrocytes the release of glutamate under ischemic and hypoxia conditions is mainly carried out through MAC channels. Using a fluorometric glutamate assay, they observed that the MAC blocker Gd^{+3} significantly decreased the glutamate release, while the VRAC blocker phloretin was less efficient in blocking glutamate release [60]. In another study, Zhao and colleagues used a luciferin–luciferase assay to study the ATP release upon incubation with glutamate in cultured astrocytes and observed that Gd^{+3} reduced the amount of ATP release but other VRAC or P2X7 blockers did not [89]. These findings highlight the potential contribution of MAC channels to ischemic injury, suggesting that these channels could be considered as novel potential targets for prevention of neuronal death in ischemia.

Although MAC channels seem to become activated primarily in the presence of toxic stimuli, such as ischemia, hypoxia, and under salt stress [2], they have been suggested to function also in physiological conditions. For example, Quasthoff and colleagues, using patch-clamp in isolated rat spinal roots, observed anion channel currents with characteristics similar to those reported for MAC and suggested a possible role of this type of channels in Schwann cells in balancing K^+ concentrations in the extracellular space of the rat spinal cord [90]. However, in this case, the role of other chloride channels cannot be ruled out, since there is no evidence of *SLCO2A1* expression in Schwann cells. Indeed, Lu and colleagues, using northern blot analysis, found that human PGT was expressed at very low levels in the adult brain. Its expression in the fetal brain was much higher though [91].

Mutations in *SLCO2A1* have been linked to some cases of pachydermoperiostosis, a rare disorder that is characterized by clubbing of the fingers, excessive sweating (hyperhidrosis), and thickening of the skin of the face [92]. In a mouse model of PGT deletion, generated by using gene targeting approaches, pups die one day after birth probably because PGT is critical for maintaining prostaglandin E2 (PGE2) concentrations during development and is needed for the closure of the ductus arteriosus [93]. Taken together, these results suggest the MAC channel might not play a key role in the function of the nervous system. However, more studies in which the MAC channels are knocked out or knocked down specifically in neurons and glia are needed. One possibility is that the MAC channels might be involved

in the regulation of ion concentration and other substances such as glutamate and ATP, therefore affecting more subtly the function of the nervous system.

The *C. elegans* gene F21G4.1 shares 28.8% of identity with *SLCO2A1* and is predicted to have sodium-independent organic anion transport activity. F21G4.1 is expressed in both glial amphid sheath and socket cells and was identified in a screen for genes that are upregulated during memory training in a CREB-dependent manner [38, 94]. Knock-down of F21G4.1 blocks long-term memory formation suggesting that glial socket cells via maxi Cl^- channels may play a role in long term memory [94]. These results are the first hint that the MAC channel in fact has a role in the physiological function of the nervous system in vivo and must be active under normal conditions. *C. elegans* represents an attractive model to further study the function of the MAC channel in glia in an in vivo context, exploiting the many advantages that this model organism offers. Another attractive genetic model is Drosophila whose genome also encodes a *SLCO2A1* homolog called Organic anion transporting polypeptide 30B (Oatp30B) of which nothing is known at this time.

10.5 Pannexins as Cl^- Channels

10.5.1 Structure and Function

Pannexins constitute another family of membrane channels expressed in glia that are permeable to Cl^- ions, at least under certain conditions. In mammals, there are three genes encoding pannexins: Panx1, 2, and 3, with Panx1 being the most studied both in vivo and in vitro. Pannexin subunits have four transmembrane domains, two short extracellular loops, and intracellular N- and C-termini. Recent structural studies have shown that Panx1 channels are heptamers [95–97], yet, previous studies have suggested that functional pannexins are formed by six subunits [98, 99]. These contrasting results suggest that techniques used in the past, often employing cross-linking agents, are prone to artifacts.

Despite their similarity with invertebrate gap junction proteins innexins, pannexins are nonjunctional membrane channels. The evidence that supports this conclusion is: first, pannexins are expressed in solitary cells such as erythrocytes; second, pannexins can be localized in nonjunctional membranes of polarized cells; third, pannexin channels are glycosylated, a post-translational modification that prevents close physical interaction which would be needed for gap-junction formation; and fourth, gap junctions formed by pannexins would physically overlap with those formed by connexins [100, 101].

The single-channel conductance and permeability properties of pannexins vary depending on the activation stimulus. Thus, pannexins have a small conductance and are permeable to Cl^- when activated by voltage (~50 pS [102, 103]) but have a large conductance (~500 pS) and are permeable to other ions as well as large endogenous molecules such as ATP and dyes when they are activated by low oxygen tension [104], mechanical forces [105], and high extracellular K^+ concentrations [106] (Fig. 10.6). A recent study has suggested that these two different pore sizes and permeability properties are the result of different channel conformations that can be reproduced by sequentially eliminating the C-terminus from each Panx1 subunit in a channel complex [108]. The same study demonstrated that a stepwise transition of the pore size can also occur via caspase 3-mediated cleavage of the C-terminus

and via activation of the α1 adrenoceptors. Recent cryo-EM studies confirm that the Panx1 channel has a large pore with a diameter of up to 30 A but with a major constriction toward the extracellular side that might account for the small conductance state [95, 96]. The small conductance Cl^--permeable state of Panx1 is activated only by strong depolarizations at membrane potentials above +20 mV [102, 103]. This requirement for activation of this state of the channel limits its physiological role. One possibility is that voltage-dependent Cl^- permeable Panx1 becomes activated during sustained depolarizations such as trains of action potential in neurons [100] or during prolonged pathological depolarizations that characterize cell death.

The permeability of Pannexins to ATP, which is associated with its higher conductance state, is relatively more understood. Indeed, this is thought to constitute the major ATP release mechanism in cells like erythrocytes that lack vesicular release [104, 109] and to contribute to ATP release in other cell types, such as epithelial cells, astrocytes, neurons, and macrophages [105, 110, 111]. Panx1 permeability to ATP is thought to be the basis of calcium waves occurring in astrocytes in vivo [112, 113].

10.5.2 Pannexins in the Nervous System of Vertebrates

Two of the three pannexins isoforms, Panx1 and Panx2, are found in the nervous system and in particular the brain ([103, 114]); however, their expression patterns do not fully overlap spatially or developmentally. Panx1 is co-expressed with Panx2 in the hippocampus, cortex, cerebellum, and olfactory bulb as shown by Bruzzone and colleagues via northern blot and in situ hybridization experiments [103]. However, the same study showed that Panx1 is the only pannexin expressed in the white matter. These data suggest that there is a possible role of Panx1, independent from Panx2, in glial cells. In another study, Vogt and colleagues, also using in situ hybridization, reported that the temporal expression patterns of Panx1 and Panx2 do not overlap in the rat brain. In particular, Panx1 is highly expressed during the embryonic and postnatal stages, while Panx2 becomes more expressed in adult brains [115]. Taken together, these findings suggest that while Panx1 and Panx2 may function in the same cells, at least in some brain regions, they also function independently and may serve overall different functions. These data also suggest that Panx1 may serve different functions in the gray (neurons) versus the white (glia) matter [116–119].

For example, Scemes and colleagues demonstrated in mice that cell-specific deletion of Panx1 in astrocytes or neurons had opposite effects on seizures induced with kainic acid [119]. In particular, mice lacking Panx1 in neurons had lower seizure score, while mice lacking Panx1 in astrocytes had worse scores, suggesting that astrocytic Panx1 is protective. The authors also showed that the amount of ATP released, upon stimulation with 10 mM KCl, was lower in mice lacking Panx1 in astrocytes. Further, using immunocytochemistry, they showed that the expression of extracellular adenosine kinase (ADK), an enzyme that regulates extracellular levels of adenosine, was higher in glial Panx1 KO mice than in wild-type mice under conditions that induce a seizure. Furthermore, inhibiting ADK improved seizure outcomes. Taken together, these results suggest that Panx1 in astrocytes regulates the ATP/adenosine balance in the microenvironment between neurons and glia resulting in effects on aberrant neuronal function in seizure. Under these conditions, Panx1

might become activated in neurons and astrocytes by either extracellular K^+ or membrane depolarization. Thus, in this case, Cl^- permeability of glial and neuronal Panx1 might have a functional significance.

Activation of Panx1 in astrocytes and neurons by high extracellular K^+ has also been linked to activation of the inflammasome, a multiprotein intracellular complex that detects pathogens and other stressors and that leads to the activation of pro-inflammatory cytokines [106]. Silverman and colleagues showed that astrocytes and neurons have an increase in caspase-1 activation and IL-1β release upon incubation with high concentrations of K^+. Using the Panx1 blocker probenicid, the investigators established that these changes were dependent on Panx1. This data underscores the role of Panx1 in inflammasome activation which normally occurs in ischemic conditions and stroke [106, 120–122]. Under these conditions, though, the low conductance Cl^- permeable Panx1 channel state is likely not present. Rather the Panx1 channel is in the higher conducting state since it displays permeability to ATP and interleukins.

While Panx1 is the most abundant pannexin in the white matter of the brain, Panx2 is expressed in astrocytes at least under pathological conditions [123]. Using immunohistochemistry, Zappala and colleagues showed that Panx2 is normally expressed in neurons of the rat hippocampus but starts to become expressed in astrocytes after ischemia. Interestingly, at the same time, the expression of Panx2 in neurons decreases. The authors suggest that astrocytic Panx2 might be involved in the release of signaling molecules in a function similar to that of Panx1. Based on what is known for Panx1, the large conductance channel is likely involved under these conditions.

10.5.3 Invertebrate Innexins

Pannexins' homologs in invertebrates are called innexins. In fact, pannexins were discovered in vertebrates following the discovery of innexins, when homologs of innexins were searched in other species [124]. The vast majority of the studies conducted so far in invertebrates, in particular in Drosophila and *C. elegans*, support that innexins function as junctional channels allowing for the passage of ions and small molecules from cell to cell [125]. However, some studies suggest that innexins may function as hemichannels.

In the leech, two types of innexins are expressed in glial cells. Both *Hm-inx2* and *Hm-inx3* are expressed in neuropil glial cells and in the packet and connective macroglia [126]. A study employing the innexin/pannexin blocker carbenoxelon and *Hm-inx2* RNAi showed that *Hm-inx2* functions as hemichannels and releases ATP in the nervous system of the leech following nerve crush injury. ATP released by *Hm-inx2* in turn activates microglial cells and promotes their migration towards the injury site. This study, though, does not address whether *Hm-inx2* functions also as a small Cl^- conductance in the nervous system of the leech [127].

In *C. elegans*, we have previously published that innexins function as mechanosensitive large-conductance hemichannels (up to 2 nS) on the plasma membrane of touch neurons cultured in vitro and in situ in living worms [128]. Using a model of chemically induced ischemia and innexin blockers probenecid and brilliant blue G (BBG), we also showed

that these innexin hemichannels promote cell death most likely functioning in their large conductance mode. However, in our electrophysiological recordings, we also found that innexins function as small conductance channels (63 pS) that can be induced to transition into large conductance state by the application of mechanical forces. Similar to the small Cl^- conductance of pannexins, the small innexin conductance we observed in *C. elegans* touch neurons is voltage-dependent and is activated by depolarizations above +20 mV. No experiments were specifically performed to address the role of this small conductance state in the physiology of touch neurons. Among the many innexins in this model organism, only INX-5 seems to be expressed almost exclusively in glial cells [129, 130]. In the future, it would be important to address the role of this glial innexin, especially its smaller Cl^- permeability state, using the wealth of genetic and molecular tools available in *C. elegans*.

10.6 Bestrophins

10.6.1 Structure and Function

Bestrophins are subunits of a family of Ca^{2+}-activated C^- channels involved in many physiological processes. In humans, bestrophins include four homologous proteins (Best1-4) encoded by the Vitelliform Macular Dystrophy (VMD) genes [131]. Interestingly, both the Drosophila and *C. elegans* genomes encode 25 genes homolog to bestrophins, perhaps suggesting that functional specificity in these invertebrates is achieved via expression of different bestrophin isoforms [131].

Human bestrophins contain between 473 and 668 amino acids and are predicted to have four α-helical transmembrane domains, with N and C termini protruding intracellularly (Fig. 10.7a). While the N-terminal region of bestrophins is highly conserved across species, the C- terminal tail is characterized by low sequence homology. Recent crystallographic studies of chicken Best1 and prokaryotic Klebsiella Pneumoniae Best revealed that this channel is barrel-shaped and is composed of five subunits positioned around a central pore. The pore is wider at the extracellular and intracellular entrances and constricts halfway through the membrane [134, 135]. A fundamental component of the bestrophin channel is the Ca^{2+} clasp, which corresponds to the Ca^{2+} binding site. The Ca^{2+} clasp is formed by a cluster of acidic residues spanning the fourth transmembrane domain and the helix-turn-helix motif in the first transmembrane domain of two adjacent subunits (in chicken Best1: Glu 300, Asp 301, Asp 302, Asp 303, and Asp 304).

Electrophysiological studies in heterologous expression systems have elucidated the basic functional properties of bestrophins. Sun and colleagues found that bestrophin channels are permeable to Cl^- ions and other anionic species by performing whole-cell recordings on human embryonic kidney cells (HEK 293) transfected with human (hBest1 and hBEST2), drosophila (dmBest1) and *C. elegans* (ceBest1) bestrophin cDNA [136]. With a pipette solution containing 148 mM CsCl, all forms of bestrophin channels displayed a reversal potential close to 0 independent of extracellular Na^+ concentration, which suggested that the current carried by the bestrophins is not generated by the movement of cations. Moreover, the fact that the reversal potential became more positive after the substitution of CsCl with gluconate was highly indicative of Cl^- conductance. The study by Sun and colleagues also showed that bestrophins' gating mechanism depends on intracellular Ca^{2+} and it is only

slightly sensitive to voltage changes (Fig. 10.7b, c). To test for Ca^{2+} dependence, the authors used a photolyzable caged calcium compound called NPEGTA. Whole-cell recordings conducted during the application of voltage pulses in the presence or absence of a flash of light showed a ~6-fold increase in the current amplitude after the flash of light delivery, while the current did not change if a Ca^{2+} chelator was administered. Similar results were obtained later including using chicken Best1 reconstituted in lipid bilayers [134]. The study in lipid bilayers supports that bestrophins' Ca^{2+} dependent gating is an intrinsic property of the channel and it is not conferred by accessory subunits or associated proteins [134].

A second mechanism of regulation of Best channels is cell volume. Fischmeister and Hartzell showed that hBest1 and mBest2 from different cell lines are sensitive to changes in osmolarity. For example, they showed that a 20% increase in extracellular osmolarity leads to 70–80% reduction in bestrophin current [137]. On the contrary, hypo-osmolarity caused an increase in current amplitude, although the effect in this case was not as strong. However, the sensitivity of bestrophins to cell volume and their involvement in the regulation of cell volume including RVD have been controversial. Indeed, peritoneal cells from BEST1/BEST2 null mice were shown to have normal volume-activated anion currents (VRAC) [138]. A more recent study though has shown that BEST1 in fact underlies the VRAC current in in mouse sperm and human retinal pigmental epithelium (RPE) cells and that best1 null mice have severe male infertility [139]. Furthermore, RPE cells derived from patients expressing mutant forms of BEST1 (BEST1-A243V; BEST1-Q238R) show reduced VRAC and RVD function [139]. Taken together, these reports seem to support regulation of bestrophin currents by cell volume and in turn involvement of these Cl^- channels in RVD, at least in some tissues.

10.6.2 Bestrophins in the Mammalian Nervous System

The expression pattern of bestrophins has been determined using PCR, immunochemical, and electrophysiological methods. One of the early studies by Marquardt and colleagues showed that Best1 was highly expressed in the retinal pigmented epithelium (RPE) in humans [140]. Similarly, Petrukhin and colleagues, also using RT-PCR and in situ hybridization, found that Best1 was highly expressed in RPE but also detected Best1 in the brain, testis, and spinal cord [141]. The expression of Best1 in RPE is preserved also in cell lines derived from this tissue as shown by Marmorstein and colleagues [142]. Outside the retina, Best1 was shown, by a combination of RT-PCR, Western Blot analysis and immunohistochemistry, to be expressed in the mouse trachea, human airway epithelial cells, mouse colon, mouse kidney, and in a mouse kidney epithelial cell line [143].

Electrophysiological experiments on mouse dorsal root ganglia (DRG) demonstrated the presence of a Ca^{2+}-dependent Cl^- current with properties resembling bestrophins [144]. Interestingly, the current was present only in medium-diameter (30–40 μm) neurons in control mice but became prominent also in large-diameter (40–50 μm) neurons in mice that had undergone transection of the sciatic nerve, suggesting ectopic upregulation of Best1 gene expression in these pathological conditions. Following these findings, RT-PCR and in situ hybridization studies showed that, although DRG neurons express three types of calcium-activated Cl^- channels (besthrophins, maxi-Cl channels, and TMEM16),

Best1 is the only one that becomes upregulated after nerve injury [145]. Indeed, using electrophysiology, Best1 siRNA, and expression of Best1 mutants, Boudes and colleagues showed that Best1 underlies that Ca^{2+}-activated Cl^- current that becomes upregulated in large diameter neurons following nerve injury [146]. The authors speculate that Best1 might be involved in the regeneration of sensory neurons after injury. Pineda-Farias and colleagues also found upregulation of Best1 in DRG neurons of a neuropathic rat model [147].

Murine Best1 has also been found in the brain in both neurons and astrocytes [148]. Brain regions that showed particularly high expression were the olfactory bulb, the hippocampus, and the cerebellum. Park and colleagues showed the expression of Best1 in both neurons and astrocytes using single-cell RT-PCR and immunohistochemistry. Furthermore, using electrophysiology, the investigators characterized Best1 currents in the hippocampal astrocytes of CA1 stratum radiatum region. They showed that a Cl^- current with features resembling bestrophins was activated by an increase in intracellular Ca^{2+} following activation of G-protein coupled receptor PAR1. Moreover, they showed that this current was reduced after silencing mBest1 gene by shRNA. Another study employing RT-PCR and shRNA silencing provided additional evidence of mBest1 expression in cortical astrocytes [149].

Later studies using immunochemical approaches combined with electron microscopy revealed that Best1 is localized in the perisynaptic astrocytic microdomains at least in the hippocampal CA1 region of the mouse (Fig. 10.8a, b) [68, 151]. Given that Best1 is enriched in these regions and shows low levels of expression in the astrocytes' soma and processes, the authors speculate that Best1 may hold an important role in the regulation of glutamate concentration at the synapses, being Best1 a possible supply of glutamate release. In support of these conclusions are the results of a study conducted in a mouse model of Alzheimer's disease (APP/PS1) [152]. The authors of this study found that in this model Best1 is not localized in perisynaptic domains but rather it is found in abundance in the hippocampal astrocytes' cell body and processes. The authors suggest that the mislocalization of Best1 might be the result of astrocytes' reactivity, a feature of astrocytes associated with several neurological and psychiatric disorders including Alzheimer's, Parkinson's, schizophrenia, and addictive disorders [153, 154].

Interestingly, in the cerebellum, Best1 is not perisynaptic, but rather in the cell body and processes of another type of glia, the Bergman glia [150, 155, 156] (Fig. 10.8d, e). This difference in protein distribution between the hippocampal astrocytes and Bergman glia accounts for the shift in the reversal potential of the currents that Park and colleagues noticed in hippocampal astrocytes when performing whole-cell recordings (Fig. 10.8c, f) [150]. Indeed, in these cells, the reversal potential was 40 mV more negative than expected under those experimental conditions, which could be explained by space clamping issues that occur when the channels are not localized in the cell body. On the contrary, in Bergman cells, the reversal potential of the ionic currents was exactly as expected, supporting that in these cells Best1 is localized in the cell body. The investigators speculate that this striking difference in the localization of Best1 between the hippocampus and the cerebellum might highlight different functions. Indeed, Best1 in the cerebellum mediates tonic inhibition by

releasing GABA, while in the hippocampus Best1 may release glutamate at the synapses [156].

As already hinted above, in addition to small anions, other anionic species permeate through bestrophin channels. For example, Qu and Hartzell using patch-clamp electrophysiology showed that all four human bestrophins and a mouse BEST2 [157] are highly permeable to $HCO3^{-}$ both at high and at physiological concentrations of this ion. These results suggest that bestrophins might participate to pH buffering in tissues. In addition to being permeable to larger anions, bestrophins are also permeable to large biologically active molecules such as glutamate and GABA, which is rather remarkable considering the size of these molecules. Park and colleagues showed in electrophysiological experiments by ion substitution method that bestrophins are permeable to glutamate, isethionate, bromine, iodine, and other small ions in mouse cultured astrocytes, with a relative permeability of glutamate to chloride ($P_{glutamate}/P_{cl}$) of 0.47 [148]. Similar permeability ratios of 0.67 and 0.53 were found for mBest1 expressed in HEK293 cells [68] and for endogenous bestrophins in CA1 hippocampal mouse astrocytes, respectively [150]. It is worth mentioning a study by Dickson and colleagues in which chicken Best1 was found to be impermeable to glutamate [134]. In this case, anionic permeability was estimated via the quenching of a fluorescent pH indicator, exploiting the fact that anionic entry into liposomes is accompanied by the entry of protons. The indirectness of the measurement may account for potential misinterpretations [158].

Among the studies investigating bestrophins' permeability to glutamate and GABA, several employed the sniffer patch-clamp technique [68, 152, 155]. This technique uses cells expressing a mutant form of GluR1 that does not get desensitized to detect glutamate released from astrocytes. This technique was developed by Lee and colleagues in a study in which they showed that astrocytic Best1, following activation of G-protein coupled receptors (GPCR), such as P2Y, bradykinin, and protease-activated receptor PAR1 (TFLLR), releases glutamate in concentrations that are sufficient for the activation of neuronal NMDRs at the synapses [159]. These results suggested that bestrophins may regulate NMDA-mediated synaptic transmission.

This hypothesis was indeed supported by Park and colleagues who showed that the release of glutamate via bestrophin channels, that are expressed in mouse hippocampal CA1 astrocytes, leads to an increase in the evoked excitatory postsynaptic potentials mediated by NMDA receptors [151]. The investigators further showed that Best1-mediated glutamate release increased the size of LTP and LTD and lowered the threshold of induction of long-term potentiation. Taken together, these results underscore that release of glutamate through Best1 expressed in astrocytes influence synaptic plasticity.

Best1 is permeable also to GABA. Lee and colleagues found a permeability ratio (P_{GABA}/P_{Cl}) of 0.27 for Best1 expressed in HEK293T cells and of 0.19 for native Best1 channels in mouse Bergmann glia [155]. Although these permeability values seem low, the investigators clarified that the current elicited by GABA permeation is carried by the less frequent anionic form of the molecule when GABA is mostly zwitterionic [158]. Interestingly, GABA release is substantial even at resting intracellular calcium concentration (100 nM), suggesting that

bestrophins could leak GABA in basal conditions. To show that GABA released via Best1 can activate GABA receptors expressed on nearby cells, Lee and colleagues used the sniffer technique which employed the slowly deactivating receptor $GABA_C$ expressed in HEK cells. Finally, the investigators, using Best1 inhibitors and shRNA against Best1, showed that in native tissue GABA released by astrocytic Best1 produces an inhibitory current in cerebellar granule cells, a finding reported also by Yoon and colleagues [156].

Importantly, while under physiological conditions GABA release via glial Best1 occurs only in the cerebellum (Bergmann glia), under pathological conditions it is released also from astrocytes. For example, Jo and colleagues showed in a mouse model of Alzheimer disease (APP/PS1) that hippocampal astrocytes in the dentate gyrus release GABA upon stimulation of the PAR-1 receptors and that the astrocytes that are closest to the plaques have the highest GABA immunoreactivity [152]. This result suggests that astrocytes reactivity may be associated with GABA production and release. Indeed, Chun and colleagues showed that a stab wound injury inflicted to the CA1 hippocampal area induced both astrocytes reactivity and an increase in GABA production and release [160].

10.6.3 Bestrophins in Invertebrates

Bestrophins have not been studied in *C. elegans* and have only been investigated by a few in Drosophila. This leaves a lot of room for exploiting these powerful model organisms to advance our understanding of the role of this family of Cl^- channels in pathophysiology, especially as it pertains to the nervous system. Drosophila Best1 has been shown to be activated by both cell swelling and Ca^{2+}, with activation by cell swelling being independent of intracellular Ca^{2+} concentrations [161]. Furthermore, Stotz and Clapham showed that the first 64 N-terminal residues of Drosphila Best1 are important for volume sensitivity and can transfer this channel feature to volume insensitive Drosophila Best2 [162]. Chien and Hartzell using a point mutation in the pore region of Drosophila Best1 (F81C) finally demonstrated that the VRAC currents resulting from expression of Best1 in S2 insect cells are mediated by Best1 and are not the result of activation of another channel for which Best1 serves as an accessory subunit [161].

Acknowledgments

I thank all the trainees and colleagues who have contributed to the work which was conducted in my laboratory and is cited in this book chapter. Work in my laboratory has been supported by the National Institute of Health (NS105616, NS106951, NS081259, NS070969, and NS049511) and the American Cancer Society (RGS-09-043-01-DDC).

References

1. Thiemann A, Grunder S, Pusch M, Jentsch TJ (1992) A chloride channel widely expressed in epithelial and non-epithelial cells. Nature 356:57–60 [PubMed: 1311421]
2. Elorza-Vidal X, Gaitan-Penas H, Estevez R (2019) Chloride channels in astrocytes: structure, roles in brain homeostasis and implications in disease. Int J Mol Sci 20
3. Hou X, Zhang R, Wang J, Li Y, Li F, Zhang Y, Zheng X, Shen Y, Wang Y, Zhou L (2018) CLC-2 is a positive modulator of oligodendrocyte precursor cell differentiation and myelination. Mol Med Rep 17:4515–4523 [PubMed: 29344669]
4. Sirisi S, Elorza-Vidal X, Arnedo T, Armand-Ugon M, Callejo G, Capdevila-Nortes X, Lopez-Hernandez T, Schulte U, Barrallo-Gimeno A, Nunes V, Gasull X, Estevez R (2017) Depolarization

causes the formation of a ternary complex between GlialCAM, MLC1 and ClC-2 in astrocytes: implications in megalencephalic leukoencephalopathy. Hum Mol Genet 26:2436–2450 [PubMed: 28398517]

5. Walz W (2002) Chloride/anion channels in glial cell membranes. Glia 40:1–10 [PubMed: 12237839]
6. Blanz J, Schweizer M, Auberson M, Maier H, Muenscher A, Hubner CA, Jentsch TJ (2007) Leukoencephalopathy upon disruption of the chloride channel ClC-2. J Neurosci 27:6581–6589 [PubMed: 17567819]
7. Lopez-Hernandez T, Sirisi S, Capdevila-Nortes X, Montolio M, Fernandez-Duenas V, Scheper GC, Van Der Knaap MS, Casquero P, Ciruela F, Ferrer I, Nunes V, Estevez R (2011) Molecular mechanisms of MLC1 and GliALCAM mutations in megalencephalic leukoencephalopathy with subcortical cysts. Hum Mol Genet 20:3266–3277 [PubMed: 21624973]
8. Hoegg-Beiler MB, Sirisi S, Orozco IJ, Ferrer I, Hohensee S, Auberson M, Godde K, Vilches C, De Heredia ML, Nunes V, Estevez R, Jentsch TJ (2014) Disrupting MLC1 and GlialCAM and ClC-2 interactions in leukodystrophy entails glial chloride channel dysfunction. Nat Commun 5:3475 [PubMed: 24647135]
9. Dutzler R (2007) A structural perspective on ClC channel and transporter function. FEBS Lett 581:2839–2844 [PubMed: 17452037]
10. Ramjeesingh M, Li C, Huan LJ, Garami E, Wang Y, Bear CE (2000) Quaternary structure of the chloride channel ClC-2. Biochemistry 39:13838–13847 [PubMed: 11076524]
11. Rinke I, Artmann J, Stein V (2010) ClC-2 voltage-gated channels constitute part of the background conductance and assist chloride extrusion. J Neurosci 30:4776–4786 [PubMed: 20357128]
12. Stolting G, Fischer M, Fahlke C (2014) ClC-1 and ClC-2 form hetero-dimeric channels with novel protopore functions. Pflugers Arch 466:2191–2204 [PubMed: 24638271]
13. Weinreich F, Jentsch TJ (2001) Pores formed by single subunits in mixed dimers of different CLC chloride channels. J Biol Chem 276:2347–2353 [PubMed: 11035003]
14. De Jesus-Perez JJ, Castro-Chong A, Shieh RC, Hernandez-Carballo CY, De Santiago-Castillo JA, Arreola J (2016) Gating the glutamate gate of CLC-2 chloride channel by pore occupancy. J Gen Physiol 147:25–37 [PubMed: 26666914]
15. Arreola J, Begenisich T, Melvin JE (2002) Conformation-dependent regulation of inward rectifier chloride channel gating by extracellular protons. J Physiol 541:103–112 [PubMed: 12015423]
16. Niemeyer MI, Yusef YR, Cornejo I, Flores CA, Sepulveda FV, Cid LP (2004) Functional evaluation of human ClC-2 chloride channel mutations associated with idiopathic generalized epilepsies. Physiol Genomics 19:74–83 [PubMed: 15252188]
17. Sanchez-Rodriguez JE, De Santiago-Castillo JA, Contreras-Vite JA, Nieto-Delgado PG, Castro-Chong A, Arreola J (2012) Sequential interaction of chloride and proton ions with the fast gate steer the voltage-dependent gating in ClC-2 chloride channels. J Physiol 590:4239–4253 [PubMed: 22753549]
18. Okada Y, Okada T, Sato-Numata K, Islam MR, Ando-Akatsuka Y, Numata T, Kubo M, Shimizu T, Kurbannazarova RS, Marunaka Y, Sabirov RZ (2019) Cell volume-activated and volume-correlated anion channels in mammalian cells: their biophysical, molecular, and pharmacological properties. Pharmacol Rev 71:49–88 [PubMed: 30573636]
19. Roman RM, Smith RL, Feranchak AP, Clayton GH, Doctor RB, Fitz JG (2001) ClC-2 chloride channels contribute to HTC cell volume homeostasis. Am J Physiol Gastrointest Liver Physiol 280:G344–G353 [PubMed: 11171616]
20. Ratte S, Prescott SA (2011) ClC-2 channels regulate neuronal excitability, not intracellular chloride levels. J Neurosci 31:15838–15843 [PubMed: 22049427]
21. Galanopoulou AS (2010) Mutations affecting GABAergic signaling in seizures and epilepsy. Pflugers Arch 460:505–523 [PubMed: 20352446]
22. Guo Z, Lu T, Peng L, Cheng H, Peng F, Li J, Lu Z, Chen S, Qiu W (2019) CLCN2-related leukoencephalopathy: a case report and review of the literature. BMC Neurol 19:156 [PubMed: 31291907]
23. Depienne C, Bugiani M, Dupuits C, Galanaud D, Touitou V, Postma N, Van Berkel C, Polder E, Tollard E, Darios F, Brice A, De Die-Smulders CE, Vles JS, Vanderver A, Uziel G, Yalcinkaya C, Frints SG, Kalscheuer VM, Klooster J, Kamermans M, Abbink TE, Wolf NI, Sedel F, Van

Der Knaap MS (2013) Brain white matter oedema due to ClC-2 chloride channel deficiency: an observational analytical study. Lancet Neurol 12:659–668 [PubMed: 23707145]

24. Estevez R, Elorza-Vidal X, Gaitan-Penas H, Perez-Rius C, Armand-Ugon M, Alonso-Gardon M, Xicoy-Espaulella E, Sirisi S, Arnedo T, Capdevila-Nortes X, Lopez-Hernandez T, Montolio M, Duarri A, Teijido O, Barrallo-Gimeno A, Palacin M, Nunes V (2018) Megalencephalic leukoencephalopathy with subcortical cysts: a personal biochemical retrospective. Eur J Med Genet 61:50–60 [PubMed: 29079544]
25. Gaitan-Penas H, Apaja PM, Arnedo T, Castellanos A, Elorza-Vidal X, Soto D, Gasull X, Lukacs GL, Estevez R (2017) Leukoencephalopathy-causing CLCN2 mutations are associated with impaired Cl(−) channel function and trafficking. J Physiol 595:6993–7008 [PubMed: 28905383]
26. Arnedo T, Aiello C, Jeworutzki E, Dentici ML, Uziel G, Simonati A, Pusch M, Bertini E, Estevez R (2014) Expanding the spectrum of megalencephalic leukoencephalopathy with subcortical cysts in two patients with GLIALCAM mutations. Neurogenetics 15:41–48 [PubMed: 24202401]
27. Perez-Rius C, Gaitan-Penas H, Estevez R, Barrallo-Gimeno A (2015) Identification and characterization of the zebrafish ClC-2 chloride channel orthologs. Pflugers Arch 467:1769–1781 [PubMed: 25236920]
28. Sik A, Smith RL, Freund TF (2000) Distribution of chloride channel-2-immunoreactive neuronal and astrocytic processes in the hippocampus. Neuroscience 101:51–65 [PubMed: 11068136]
29. Makara JK, Rappert A, Matthias K, Steinhauser C, Spat A, Kettenmann H (2003) Astrocytes from mouse brain slices express ClC-2-mediated Cl-currents regulated during development and after injury. Mol Cell Neurosci 23:521–530 [PubMed: 12932434]
30. Mladinic M, Becchetti A, Didelon F, Bradbury A, Cherubini E (1999) Low expression of the ClC-2 chloride channel during postnatal development: a mechanism for the paradoxical depolarizing action of GABA and glycine in the hippocampus. Proc Biol Sci 266:1207–1213 [PubMed: 10418163]
31. Zhao B, Quan H, Ma T, Tian Y, Cai Q, Li H (2015) 4,4′-Diisothiocyanostilbene-2,2′-disulfonic Acid (DIDS) ameliorates ischemia-hypoxia-induced white matter damage in neonatal rats through inhibition of the voltage-gated chloride channel ClC-2. Int J Mol Sci 16:10457–10469 [PubMed: 25961953]
32. He F, Peng Y, Yang Z, Ge Z, Tian Y, Ma T, Li H (2017) Activated ClC-2 Inhibits p-Akt to repress myelination in GDM newborn rats. Int J Biol Sci 13:179–188 [PubMed: 28255270]
33. Bosl MR, Stein V, Hubner C, Zdebik AA, Jordt SE, Mukhopadhyay AK, Davidoff MS, Holstein AF, Jentsch TJ (2001) Male germ cells and photoreceptors, both dependent on close cell-cell interactions, degenerate upon ClC-2 Cl(−) channel disruption. EMBO J 20:1289–1299 [PubMed: 11250895]
34. Dubey M, Bugiani M, Ridder MC, Postma NL, Brouwers E, Polder E, Jacobs JG, Baayen JC, Klooster J, Kamermans M, Aardse R, De Kock CP, Dekker MP, Van Weering JR, Heine VM, Abbink TE, Scheper GC, Boor I, Lodder JC, Mansvelder HD, Van Der Knaap MS (2015) Mice with megalencephalic leukoencephalopathy with cysts: a developmental angle. Ann Neurol 77:114–131 [PubMed: 25382142]
35. Bugiani M, Dubey M, Breur M, Postma NL, Dekker MP, Ter Braak T, Boschert U, Abbink TEM, Mansvelder HD, Min R, Van Weering JRT, Van Der Knaap MS (2017) Megalencephalic leukoencephalopathy with cysts: the Glialcam-null mouse model. Ann Clin Transl Neurol 4:450–465 [PubMed: 28695146]
36. Van Der Knaap MS, Depienne C, Sedel F, Abbink TEM (1993) CLCN2-Related leukoencephalopathy. In: Adam MP, Ardinger HH, Pagon RA, Wallace SE, Bean LJH, Stephens K, Amemiya A (eds) GeneReviews((R)), Seattle (WA)
37. Plazaola-Sasieta H, Zhu Q, Gaitan-Penas H, Rios M, Estevez R, Morey M (2019) Drosophila ClC-a is required in glia of the stem cell niche for proper neurogenesis and wiring of neural circuits. Glia 67:2374–2398 [PubMed: 31479171]
38. Grant J, Matthewman C, Bianchi L (2015) A novel mechanism of pH buffering in *C. elegans* Glia: bicarbonate transport via the voltage-gated ClC Cl− Channel CLH-1. J Neurosci 35:16377–16397 [PubMed: 26674864]

39. Sanchez-Rodriguez JE, De Santiago-Castillo JA, Arreola J (2010) Permeant anions contribute to voltage dependence of ClC-2 chloride channel by interacting with the protopore gate. J Physiol 588:2545–2556 [PubMed: 20498235]
40. Park C, Sakurai Y, Sato H, Kanda S, Iino Y, Kunitomo H (2021) Roles of the ClC Chloride Channel CLH-1 in food-associated salt chemotaxis behavior of *C. elegans*. Elife 10:e255701. 2020.02.16.951368
41. Akita T, Okada Y (2014) Characteristics and roles of the volume-sensitive outwardly rectifying (VSOR) anion channel in the central nervous system. Neuroscience 275:211–231 [PubMed: 24937753]
42. Konig B, Stauber T (2019) Biophysics and structure-function relationships of LRRC8-formed volume-regulated anion channels. Biophys J 116:1185–1193 [PubMed: 30871717]
43. Yamada T, Strange K (2018) Intracellular and extracellular loops of LRRC8 are essential for volume-regulated anion channel function. J Gen Physiol 150:1003–1015 [PubMed: 29853476]
44. Murana E, Pagani F, Basilico B, Sundukova M, Batti L, Di Angelantonio S, Cortese B, Grimaldi A, Francioso A, Heppenstall P, Bregestovski P, Limatola C, Ragozzino D (2017) ATP release during cell swelling activates a Ca(2+)-dependent Cl(−) current by autocrine mechanism in mouse hippocampal microglia. Sci Rep 7:4184 [PubMed: 28646166]
45. Schober AL, Wilson CS, Mongin AA (2017) Molecular composition and heterogeneity of the LRRC8-containing swelling-activated osmolyte channels in primary rat astrocytes. J Physiol 595:6939–6951 [PubMed: 28833202]
46. Nunez R, Sancho-Martinez SM, Novoa JM, Lopez-Hernandez FJ (2010) Apoptotic volume decrease as a geometric determinant for cell dismantling into apoptotic bodies. Cell Death Differ 17:1665–1671 [PubMed: 20706273]
47. Hoffmann EK, Sorensen BH, Sauter DP, Lambert IH (2015) Role of volume-regulated and calcium-activated anion channels in cell volume homeostasis, cancer and drug resistance. Channels (Austin) 9:380–396 [PubMed: 26569161]
48. Shimizu T, Numata T, Okada Y (2004) A role of reactive oxygen species in apoptotic activation of volume-sensitive Cl(−) channel. Proc Natl Acad Sci U S A 101:6770–6773 [PubMed: 15096609]
49. Pasantes-Morales H, Moran J, Schousboe A (1990) Volume-sensitive release of taurine from cultured astrocytes: properties and mechanism. Glia 3:427–432 [PubMed: 2146228]
50. Sanchez-Olea R, Pena C, Moran J, Pasantes-Morales H (1993) Inhibition of volume regulation and efflux of osmoregulatory amino acids by blockers of Cl-transport in cultured astrocytes. Neurosci Lett 156:141–144 [PubMed: 8414176]
51. Bakhramov A, Fenech C, Bolton TB (1995) Chloride current activated by hypotonicity in cultured human astrocytoma cells. Exp Physiol 80:373–389 [PubMed: 7543762]
52. Parkerson KA, Sontheimer H (2004) Biophysical and pharmacological characterization of hypotonically activated chloride currents in cortical astrocytes. Glia 46:419–436 [PubMed: 15095372]
53. Abdullaev IF, Rudkouskaya A, Schools GP, Kimelberg HK, Mongin AA (2006) Pharmacological comparison of swelling-activated excitatory amino acid release and Cl-currents in cultured rat astrocytes. J Physiol 572:677–689 [PubMed: 16527858]
54. Ando-Akatsuka Y, Shimizu T, Numata T, Okada Y (2012) Involvements of the ABC protein ABCF2 and alpha-actinin-4 in regulation of cell volume and anion channels in human epithelial cells. J Cell Physiol 227:3498–3510 [PubMed: 22252987]
55. Mongin AA, Kimelberg HK (2005) ATP regulates anion channel-mediated organic osmolyte release from cultured rat astrocytes via multiple Ca2+-sensitive mechanisms. Am J Physiol Cell Physiol 288:C204–C213 [PubMed: 15371260]
56. Konig B, Hao Y, Schwartz S, Plested AJ, Stauber T (2019) A FRET sensor of C-terminal movement reveals VRAC activation by plasma membrane DAG signaling rather than ionic strength. Elife 8
57. Qiu Z, Dubin AE, Mathur J, Tu B, Reddy K, Miraglia LJ, Reinhardt J, Orth AP, Patapoutian A (2014) SWELL1, a plasma membrane protein, is an essential component of volume-regulated anion channel. Cell 157:447–458 [PubMed: 24725410]

58. Voss FK, Ullrich F, Munch J, Lazarow K, Lutter D, Mah N, Andrade-Navarro MA, Von Kries JP, Stauber T, Jentsch TJ (2014) Identification of LRRC8 heteromers as an essential component of the volume-regulated anion channel VRAC. Science 344:634–638 [PubMed: 24790029]
59. Galietta LJ, Haggie PM, Verkman AS (2001) Green fluorescent protein-based halide indicators with improved chloride and iodide affinities. FEBS Lett 499:220–224 [PubMed: 11423120]
60. Liu HT, Tashmukhamedov BA, Inoue H, Okada Y, Sabirov RZ (2006) Roles of two types of anion channels in glutamate release from mouse astrocytes under ischemic or osmotic stress. Glia 54:343–357 [PubMed: 16883573]
61. Liu HT, Akita T, Shimizu T, Sabirov RZ, Okada Y (2009) Bradykinin-induced astrocyte-neuron signalling: glutamate release is mediated by ROS-activated volume-sensitive outwardly rectifying anion channels. J Physiol 587:2197–2209 [PubMed: 19188250]
62. Yang J, Vitery MDC, Chen J, Osei-Owusu J, Chu J, Qiu Z (2019b) Glutamate-releasing SWELL1 channel in astrocytes modulates synaptic transmission and promotes brain damage in stroke. Neuron 102 (813–827):e6
63. Cavelier P, Attwell D (2005) Tonic release of glutamate by a DIDS-sensitive mechanism in rat hippocampal slices. J Physiol 564:397–410 [PubMed: 15695241]
64. Le Meur K, Galante M, Angulo MC, Audinat E (2007) Tonic activation of NMDA receptors by ambient glutamate of non-synaptic origin in the rat hippocampus. J Physiol 580:373–383 [PubMed: 17185337]
65. Kimelberg HK, Goderie SK, Higman S, Pang S, Waniewski RA (1990) Swelling-induced release of glutamate, aspartate, and taurine from astrocyte cultures. J Neurosci 10:1583–1591 [PubMed: 1970603]
66. Bowens NH, Dohare P, Kuo YH, Mongin AA (2013) DCPIB, the proposed selective blocker of volume-regulated anion channels, inhibits several glutamate transport pathways in glial cells. Mol Pharmacol 83:22–32 [PubMed: 23012257]
67. Tian GF, Azmi H, Takano T, Xu Q, Peng W, Lin J, Oberheim N, Lou N, Wang X, Zielke HR, Kang J, Nedergaard M (2005) An astrocytic basis of epilepsy. Nat Med 11:973–981 [PubMed: 16116433]
68. Woo DH, Han KS, Shim JW, Yoon BE, Kim E, Bae JY, Oh SJ, Hwang EM, Marmorstein AD, Bae YC, Park JY, Lee CJ (2012) TREK-1 and Best1 channels mediate fast and slow glutamate release in astrocytes upon GPCR activation. Cell 151:25–40 [PubMed: 23021213]
69. Capurro V, Gianotti A, Caci E, Ravazzolo R, Galietta LJ, Zegarra-Moran O (2015) Functional analysis of acid-activated Cl(−) channels: properties and mechanisms of regulation. Biochim Biophys Acta 1848:105–114 [PubMed: 25306966]
70. Lambert S, Oberwinkler J (2005) Characterization of a proton-activated, outwardly rectifying anion channel. J Physiol 567:191–213 [PubMed: 15961423]
71. Auzanneau C, Thoreau V, Kitzis A, Becq F (2003) A Novel voltage-dependent chloride current activated by extracellular acidic pH in cultured rat Sertoli cells. J Biol Chem 278:19230–19236 [PubMed: 12637509]
72. Fu ZJ, Li XZ, Wang QR, Shi L, Zhang LQ, Pan XL (2013) Extracellular acidic pH-activated, outward rectifying chloride currents can be regulated by reactive oxygen species in human THP-1 monocytes. Biochem Biophys Res Commun 432:701–706 [PubMed: 23376719]
73. Matsuda JJ, Filali MS, Collins MM, Volk KA, Lamb FS (2010) The ClC-3 Cl−/H+ antiporter becomes uncoupled at low extracellular pH. J Biol Chem 285:2569–2579 [PubMed: 19926787]
74. Wang HY, Shimizu T, Numata T, Okada Y (2007) Role of acid-sensitive outwardly rectifying anion channels in acidosis-induced cell death in human epithelial cells. Pflugers Arch 454:223–233 [PubMed: 17186306]
75. Sato-Numata K, Numata T, Inoue R, Okada Y (2016) Distinct pharmacological and molecular properties of the acid-sensitive outwardly rectifying (ASOR) anion channel from those of the volume-sensitive outwardly rectifying (VSOR) anion channel. Pflugers Arch 468:795–803 [PubMed: 26743872]
76. Kittl M, Helm K, Beyreis M, Mayr C, Gaisberger M, Winklmayr M, Ritter M, Jakab M (2019) Acid- and volume-sensitive chloride currents in microglial cells. Int J Mol Sci 20

77. Ullrich F, Blin S, Lazarow K, Daubitz T, Von Kries JP, Jentsch TJ (2019) Identification of TMEM206 proteins as pore of PAORAC/ASOR acid-sensitive chloride channels. Elife 8:e49187 [PubMed: 31318332]

78. Yang J, Chen J, Del Carmen Vitery M, Osei-Owusu J, Chu J, Yu H, Sun S, Qiu Z (2019a) PAC, an evolutionary conserved membrane protein, is a proton-activated chloride channel. Science 364:395–399 [PubMed: 31023925]

79. Osei-Owusu J, Yang J, Del Carmen Vitery M, Tian M, Qiu Z (2020) PAC proton-activated chloride channel contributes to acid-induced cell death in primary rat cortical neurons. Channels (Austin) 14:53–58 [PubMed: 32093550]

80. Gray PT, Bevan S, Ritchie JM (1984) High conductance anion-selective channels in rat cultured Schwann cells. Proc R Soc Lond B Biol Sci 221:395–409 [PubMed: 6146983]

81. Jalonen T (1993) Single-channel characteristics of the large-conductance anion channel in rat cortical astrocytes in primary culture. Glia 9:227–237 [PubMed: 7507468]

82. Nowak L, Ascher P, Berwald-Netter Y (1987) Ionic channels in mouse astrocytes in culture. J Neurosci 7:101–109 [PubMed: 2433415]

83. Sonnhof U (1987) Single voltage-dependent K+ and Cl− channels in cultured rat astrocytes. Can J Physiol Pharmacol 65:1043–1050 [PubMed: 2441828]

84. Hazama A, Fan HT, Abdullaev I, Maeno E, Tanaka S, Ando-Akatsuka Y, Okada Y (2000) Swelling-activated, cystic fibrosis transmembrane conductance regulator-augmented ATP release and Cl− conductances in murine C127 cells. J Physiol 523(Pt 1):1–11 [PubMed: 10673540]

85. Islam MR, Uramoto H, Okada T, Sabirov RZ, Okada Y (2012) Maxi-anion channel and pannexin 1 hemichannel constitute separate pathways for swelling-induced ATP release in murine L929 fibrosarcoma cells. Am J Physiol Cell Physiol 303:C924–C935 [PubMed: 22785119]

86. Toychiev AH, Sabirov RZ, Takahashi N, Ando-Akatsuka Y, Liu H, Shintani T, Noda M, Okada Y (2009) Activation of maxi-anion channel by protein tyrosine dephosphorylation. Am J Physiol Cell Physiol 297:C990–C1000 [PubMed: 19657061]

87. Bosma MM (1989) Anion channels with multiple conductance levels in a mouse B lymphocyte cell line. J Physiol 410:67–90 [PubMed: 2477528]

88. Sabirov RZ, Merzlyak PG, Okada T, Islam MR, Uramoto H, Mori T, Makino Y, Matsuura H, Xie Y, Okada Y (2017) The organic anion transporter SLCO2A1 constitutes the core component of the Maxi-Cl channel. EMBO J 36:3309–3324 [PubMed: 29046334]

89. Zhao B, Gu L, Liu K, Zhang M, Liu H (2017) Maxi-anion channels play a key role in glutamate-induced ATP release from mouse astrocytes in primary culture. Neuroreport 28:380–385 [PubMed: 28257396]

90. Quasthoff S, Strupp M, Grafe P (1992) High conductance anion channel in Schwann cell vesicles from rat spinal roots. Glia 5:17–24 [PubMed: 1371762]

91. Lu R, Kanai N, Bao Y, Schuster VL (1996) Cloning, in vitro expression, and tissue distribution of a human prostaglandin transporter cDNA(hPGT). J Clin Invest 98:1142–1149 [PubMed: 8787677]

92. Diggle CP, Parry DA, Logan CV, Laissue P, Rivera C, Restrepo CM, Fonseca DJ, Morgan JE, Allanore Y, Fontenay M, Wipff J, Varret M, Gibault L, Dalantaeva N, Korbonits M, Zhou B, Yuan G, Harifi G, Cefle K, Palanduz S, Akoglu H, Zwijnenburg PJ, Lichtenbelt KD, Aubry-Rozier B, Superti-Furga A, Dallapiccola B, Accadia M, Brancati F, Sheridan EG, Taylor GR, Carr IM, Johnson CA, Markham AF, Bonthron DT (2012) Prostaglandin transporter mutations cause pachydermoperiostosis with myelofibrosis. Hum Mutat 33:1175–1181 [PubMed: 22553128]

93. Chang HY, Locker J, Lu R, Schuster VL (2010) Failure of postnatal ductus arteriosus closure in prostaglandin transporter-deficient mice. Circulation 121:529–536 [PubMed: 20083684]

94. Lakhina V, Arey RN, Kaletsky R, Kauffman A, Stein G, Keyes W, Xu D, Murphy CT (2015) Genome-wide functional analysis of CREB/long-term memory-dependent transcription reveals distinct basal and memory gene expression programs. Neuron 85:330–345 [PubMed: 25611510]

95. Deng Z, He Z, Maksaev G, Bitter RM, Rau M, Fitzpatrick JAJ, Yuan P (2020) Cryo-EM structures of the ATP release channel pannexin 1. Nat Struct Mol Biol 27:373–381 [PubMed: 32231289]

96. Michalski K, Syrjanen JL, Henze E, Kumpf J, Furukawa H, Kawate T (2020) The Cryo-EM structure of pannexin 1 reveals unique motifs for ion selection and inhibition. Elife 9

97. Mou L, Ke M, Song M, Shan Y, Xiao Q, Liu Q, LI J, Sun K, Pu L, Guo L, Geng J, Wu J, Deng D (2020) Structural basis for gating mechanism of Pannexin 1 channel. Cell Res 30:452–454 [PubMed: 32284561]

98. Boassa D, Ambrosi C, Qiu F, Dahl G, Gaietta G, Sosinsky G (2007) Pannexin1 channels contain a glycosylation site that targets the hexamer to the plasma membrane. J Biol Chem 282:31733–31743 [PubMed: 17715132]

99. Boassa D, Qiu F, Dahl G, Sosinsky G (2008) Trafficking dynamics of glycosylated pannexin 1 proteins. Cell Commun Adhes 15:119–132 [PubMed: 18649184]

100. Dahl G (2018) The Pannexin1 membrane channel: distinct conformations and functions. FEBS Lett 592:3201–3209 [PubMed: 29802622]

101. Penuela S, Bhalla R, Gong XQ, Cowan KN, Celetti SJ, Cowan BJ, Bai D, Shao Q, Laird DW (2007) Pannexin 1 and pannexin 3 are glycoproteins that exhibit many distinct characteristics from the connexin family of gap junction proteins. J Cell Sci 120:3772–3783 [PubMed: 17925379]

102. Bao L, Locovei S, Dahl G (2004) Pannexin membrane channels are mechanosensitive conduits for ATP. FEBS Lett 572:65–68 [PubMed: 15304325]

103. Bruzzone R, Hormuzdi SG, Barbe MT, Herb A, Monyer H (2003) Pannexins, a family of gap junction proteins expressed in brain. Proc Natl Acad Sci U S A 100:13644–13649 [PubMed: 14597722]

104. Sridharan M, Adderley SP, Bowles EA, Egan TM, Stephenson AH, Ellsworth ML, Sprague RS (2010) Pannexin 1 is the conduit for low oxygen tension-induced ATP release from human erythrocytes. Am J Physiol Heart Circ Physiol 299:H1146–H1152 [PubMed: 20622111]

105. Ransford GA, Fregien N, Qiu F, Dahl G, Conner GE, Salathe M (2009) Pannexin 1 contributes to ATP release in airway epithelia. Am J Respir Cell Mol Biol 41:525–534 [PubMed: 19213873]

106. Silverman WR, De Rivero Vaccari JP, Locovei S, Qiu F, Carlsson SK, Scemes E, Keane RW, Dahl G (2009) The pannexin 1 channel activates the inflammasome in neurons and astrocytes. J Biol Chem 284:18143–18151 [PubMed: 19416975]

107. Wang J, Ambrosi C, Qiu F, Jackson DG, Sosinsky G, Dahl G (2014) The membrane protein Pannexin1 forms two open-channel conformations depending on the mode of activation. Sci Signal 7:ra69 [PubMed: 25056878]

108. Chiu YH, Jin X, Medina CB, Leonhardt SA, Kiessling V, Bennett BC, Shu S, Tamm LK, Yeager M, Ravichandran KS, Bayliss DA (2017) A quantized mechanism for activation of pannexin channels. Nat Commun 8:14324 [PubMed: 28134257]

109. Locovei S, Bao L, Dahl G (2006a) Pannexin 1 in erythrocytes: Function without a gap. Proc Natl Acad Sci U S A 103:7655–7659 [PubMed: 16682648]

110. Dahl G (2015) ATP release through pannexon channels. Philos Trans R Soc Lond B Biol Sci 370

111. Qu Y, Misaghi S, Newton K, Gilmour LL, Louie S, Cupp JE, Dubyak GR, Hackos D, Dixit VM (2011) Pannexin-1 is required for ATP release during apoptosis but not for inflammasome activation. J Immunol 186:6553–6561 [PubMed: 21508259]

112. Locovei S, Wang J, Dahl G (2006b) Activation of pannexin 1 channels by ATP through P2Y receptors and by cytoplasmic calcium. FEBS Lett 580:239–244 [PubMed: 16364313]

113. Suadicani SO, Iglesias R, Wang J, Dahl G, Spray DC, Scemes E (2012) ATP signaling is deficient in cultured Pannexin1-null mouse astrocytes. Glia 60:1106–1116 [PubMed: 22499153]

114. Baranova A, Ivanov D, Petrash N, Pestova A, Skoblov M, Kelmanson I, Shagin D, Nazarenko S, Geraymovych E, Litvin O, Tiunova A, Born TL, Usman N, Staroverov D, Lukyanov S, Panchin Y (2004) The mammalian pannexin family is homologous to the invertebrate innexin gap junction proteins. Genomics 83:706–716 [PubMed: 15028292]

115. Vogt A, Hormuzdi SG, Monyer H (2005) Pannexin1 and Pannexin2 expression in the developing and mature rat brain. Brain Res Mol Brain Res 141:113–120 [PubMed: 16143426]

116. Bennett MV, Garre JM, Orellana JA, Bukauskas FF, Nedergaard M, Saez JC (2012) Connexin and pannexin hemichannels in inflammatory responses of glia and neurons. Brain Res 1487:3–15 [PubMed: 22975435]

117. Hanstein R, Hanani M, Scemes E, Spray DC (2016) Glial pannexin1 contributes to tactile hypersensitivity in a mouse model of orofacial pain. Sci Rep 6:38266 [PubMed: 27910899]

118. Sanderson J, Dartt DA, Trinkaus-Randall V, Pintor J, Civan MM, Delamere NA, Fletcher EL, Salt TE, Grosche A, Mitchell CH (2014) Purines in the eye: recent evidence for the physiological and pathological role of purines in the RPE, retinal neurons, astrocytes, Muller cells, lens, trabecular meshwork, cornea and lacrimal gland. Exp Eye Res 127:270–279 [PubMed: 25151301]
119. Scemes E, Velisek L, Veliskova J (2019) Astrocyte and neuronal pannexin1 contribute distinctly to seizures. ASN Neuro 11:1759091419833502 [PubMed: 30862176]
120. Adamson SE, Leitinger N (2014) The role of pannexin1 in the induction and resolution of inflammation. FEBS Lett 588:1416–1422 [PubMed: 24642372]
121. Crespo Yanguas S, Willebrords J, Johnstone SR, Maes M, Decrock E, De Bock M, Leybaert L, Cogliati B, Vinken M (2017) Pannexin1 as mediator of inflammation and cell death. Biochim Biophys Acta Mol Cell Res 1864:51–61 [PubMed: 27741412]
122. Pelegrin P, Surprenant A (2006) Pannexin-1 mediates large pore formation and interleukin-1beta release by the ATP-gated P2X7 receptor. Embo J 25:5071–5082 [PubMed: 17036048]
123. Zappala A, Li Volti G, Serapide MF, Pellitteri R, Falchi M, La Delia F, Cicirata V, Cicirata F (2007) Expression of pannexin2 protein in healthy and ischemized brain of adult rats. Neuroscience 148:653–667 [PubMed: 17692470]
124. Panchin Y, Kelmanson I, Matz M, Lukyanov K, Usman N, Lukyanov S (2000) A ubiquitous family of putative gap junction molecules. Curr Biol 10:R473–R474 [PubMed: 10898987]
125. Sanchez A, Castro C, Flores DL, Gutierrez E, Baldi P (2019) Gap junction channels of innexins and connexins: relations and computational perspectives. Int J Mol Sci 20
126. Dykes IM, Macagno ER (2006) Molecular characterization and embryonic expression of innexins in the leech Hirudo medicinalis. Dev Genes Evol 216:185–197 [PubMed: 16440200]
127. Samuels SE, Lipitz JB, Dahl G, Muller KJ (2010) Neuroglial ATP release through innexin channels controls microglial cell movement to a nerve injury. J Gen Physiol 136:425–442 [PubMed: 20876360]
128. Sangaletti R, Dahl G, Bianchi L (2014) Mechanosensitive unpaired innexin channels in C. elegans touch neurons. Am J Physiol Cell Physiol 307:C966–C977 [PubMed: 25252948]
129. Altun ZF, Chen B, Wang ZW, Hall DH (2009) High resolution map of Caenorhabditis elegans gap junction proteins. Dev Dyn 238:1936–1950 [PubMed: 19621339]
130. Hall DH (2017) Gap junctions in *C. elegans*: their roles in behavior and development. Dev Neurobiol 77:587–596 [PubMed: 27294317]
131. Hartzell HC, Qu Z, Yu K, Xiao Q, Chien LT (2008) Molecular physiology of bestrophins: multifunctional membrane proteins linked to best disease and other retinopathies. Physiol Rev 88:639–672 [PubMed: 18391176]
132. Milenkovic VM, Rivera A, Horling F, Weber BH (2007) Insertion and topology of normal and mutant bestrophin-1 in the endoplasmic reticulum membrane. J Biol Chem 282:1313–1321 [PubMed: 17110374]
133. Li Y, Zhang Y, Xu Y, Kittredge A, Ward N, Chen S, Tsang SH, Yang T (2017) Patient-specific mutations impair BESTROPHIN1's essential role in mediating Ca(2+)-dependent Cl(−) currents in human RPE. Elife 6
134. Kane Dickson V, Pedi L, Long SB (2014) Structure and insights into the function of a Ca(2+)-activated Cl(−) channel. Nature 516:213–218 [PubMed: 25337878]
135. Yang T, Liu Q, Kloss B, Bruni R, Kalathur RC, Guo Y, Kloppmann E, Rost B, Colecraft HM, Hendrickson WA (2014) Structure and selectivity in bestrophin ion channels. Science 346:355–359 [PubMed: 25324390]
136. Sun H, Tsunenari T, Yau KW, Nathans J (2002) The vitelliform macular dystrophy protein defines a new family of chloride channels. Proc Natl Acad Sci U S A 99:4008–4013 [PubMed: 11904445]
137. Fischmeister R, Hartzell HC (2005) Volume sensitivity of the bestrophin family of chloride channels. J Physiol 562:477–491 [PubMed: 15564283]
138. Chien LT, Hartzell HC (2008) Rescue of volume-regulated anion current by bestrophin mutants with altered charge selectivity. J Gen Physiol 132:537–546 [PubMed: 18955594]

139. Milenkovic A, Schmied D, Tanimoto N, Seeliger MW, Sparrow JR, Weber BHF (2019) The Y227N mutation affects bestrophin-1 protein stability and impairs sperm function in a mouse model of Best vitelliform macular dystrophy. Biol Open 8
140. Marquardt A, Stohr H, Passmore LA, Kramer F, Rivera A, Weber BH (1998) Mutations in a novel gene, VMD2, encoding a protein of unknown properties cause juvenile-onset vitelliform macular dystrophy (Best's disease). Hum Mol Genet 7:1517–1525 [PubMed: 9700209]
141. Petrukhin K, Koisti MJ, Bakall B, Li W, Xie G, Marknell T, Sandgren O, Forsman K, Holmgren G, Andreasson S, Vujic M, Bergen AA, Mcgarty-Dugan V, Figueroa D, Austin CP, Metzker ML, Caskey CT, Wadelius C (1998) Identification of the gene responsible for Best macular dystrophy. Nat Genet 19:241–247 [PubMed: 9662395]
142. Marmorstein AD, Marmorstein LY, Rayborn M, Wang X, Hollyfield JG, Petrukhin K (2000) Bestrophin, the product of the Best vitelliform macular dystrophy gene (VMD2), localizes to the basolateral plasma membrane of the retinal pigment epithelium. Proc Natl Acad Sci U S A 97:12758–12763 [PubMed: 11050159]
143. Barro Soria R, Spitzner M, Schreiber R, Kunzelmann K (2009) Bestrophin-1 enables Ca2+-activated Cl-conductance in epithelia. J Biol Chem 284:29405–29412 [PubMed: 17003041]
144. Andre S, Boukhaddaoui H, Campo B, Al-Jumaily M, Mayeux V, Greuet D, Valmier J, Scamps F (2003) Axotomy-induced expression of calcium-activated chloride current in subpopulations of mouse dorsal root ganglion neurons. J Neurophysiol 90:3764–3773 [PubMed: 12944538]
145. Al-Jumaily M, Kozlenkov A, Mechaly I, Fichard A, Matha V, Scamps F, Valmier J, Carroll P (2007) Expression of three distinct families of calcium-activated chloride channel genes in the mouse dorsal root ganglion. Neurosci Bull 23:293–299 [PubMed: 17952139]
146. Boudes M, Sar C, Menigoz A, Hilaire C, Pequignot MO, Kozlenkov A, Marmorstein A, Carroll P, Valmier J, Scamps F (2009) Best1 is a gene regulated by nerve injury and required for Ca2+-activated Cl-current expression in axotomized sensory neurons. J Neurosci 29:10063–10071 [PubMed: 19675239]
147. Pineda-Farias JB, Barragan-Iglesias P, Loeza-Alcocer E, Torres-Lopez JE, Rocha-Gonzalez HI, Perez-Severiano F, Delgado-Lezama R, Granados-Soto V (2015) Role of anoctamin-1 and bestrophin-1 in spinal nerve ligation-induced neuropathic pain in rats. Mol Pain 11:41 [PubMed: 26130088]
148. Park H, Oh SJ, Han KS, Woo DH, Park H, Mannaioni G, Traynelis SF, Lee CJ (2009) Bestrophin-1 encodes for the Ca2+-activated anion channel in hippocampal astrocytes. J Neurosci 29:13063–13073 [PubMed: 19828819]
149. Oh SJ, Han KS, Park H, Woo DH, Kim HY, Traynelis SF, Lee CJ (2012) Protease activated receptor 1-induced glutamate release in cultured astrocytes is mediated by Bestrophin-1 channel but not by vesicular exocytosis. Mol Brain 5:38 [PubMed: 23062602]
150. Park H, Han KS, Oh SJ, Jo S, Woo J, Yoon BE, Lee CJ (2013) High glutamate permeability and distal localization of Best1 channel in CA1 hippocampal astrocyte. Mol Brain 6:54 [PubMed: 24321245]
151. Park H, Han KS, Seo J, Lee J, Dravid SM, Woo J, Chun H, Cho S, Bae JY, An H, Koh W, Yoon BE, Berlinguer-Palmini R, Mannaioni G, Traynelis SF, Bae YC, Choi SY, Lee CJ (2015) Channel-mediated astrocytic glutamate modulates hippocampal synaptic plasticity by activating postsynaptic NMDA receptors. Mol Brain 8:7 [PubMed: 25645137]
152. Jo S, Yarishkin O, Hwang YJ, Chun YE, Park M, Woo DH, Bae JY, Kim T, Lee J, Chun H, Park HJ, Lee DY, Hong J, Kim HY, Oh SJ, Park SJ, Lee H, Yoon BE, Kim Y, Jeong Y, Shim I, Bae YC, Cho J, Kowall NW, Ryu H, Hwang E, Kim D, Lee CJ (2014) GABA from reactive astrocytes impairs memory in mouse models of Alzheimer's disease. Nat Med 20:886–896 [PubMed: 24973918]
153. Miguel-Hidalgo JJ (2009) The role of glial cells in drug abuse. Curr Drug Abuse Rev 2:76–82 [PubMed: 19606280]
154. Tarasov VV, Svistunov AA, Chubarev VN, Sologova SS, Mukhortova P, Levushkin D, Somasundaram SG, Kirkland CE, Bachurin SO, Aliev G (2019) Alterations of astrocytes in the context of schizophrenic dementia. Front Pharmacol 10:1612 [PubMed: 32116664]

155. Lee S, Yoon BE, Berglund K, Oh SJ, Park H, Shin HS, Augustine GJ, Lee CJ (2010) Channel-mediated tonic GABA release from glia. Science 330:790–796 [PubMed: 20929730]

156. Yoon BE, Jo S, Woo J, Lee JH, Kim T, Kim D, Lee CJ (2011) The amount of astrocytic GABA positively correlates with the degree of tonic inhibition in hippocampal CA1 and cerebellum. Mol Brain 4:42 [PubMed: 22107761]

157. Qu Z, Hartzell HC (2008) Bestrophin Cl− channels are highly permeable to HCO3. Am J Physiol Cell Physiol 294:C1371–C1377 [PubMed: 18400985]

158. Oh SJ, Lee CJ (2017) Distribution and function of the bestrophin-1 (Best1) channel in the brain. Exp Neurobiol 26:113–121 [PubMed: 28680296]

159. Lee CJ, Mannaioni G, Yuan H, Woo DH, Gingrich MB, Traynelis SF (2007) Astrocytic control of synaptic NMDA receptors. J Physiol 581:1057–1081 [PubMed: 17412766]

160. Chun H, An H, Lim J, Woo J, Lee J, Ryu H, Lee CJ (2018) Astrocytic proBDNF and Tonic GABA distinguish active versus reactive astrocytes in hippocampus. Exp Neurobiol 27:155–170 [PubMed: 30022867]

161. Chien LT, Hartzell HC (2007) Drosophila bestrophin-1 chloride current is dually regulated by calcium and cell volume. J Gen Physiol 130:513–524 [PubMed: 17968025]

162. Stotz SC, Clapham DE (2012) Anion-sensitive fluorophore identifies the Drosophila swell-activated chloride channel in a genome-wide RNA interference screen. PLoS One 7:e46865 [PubMed: 23056495]

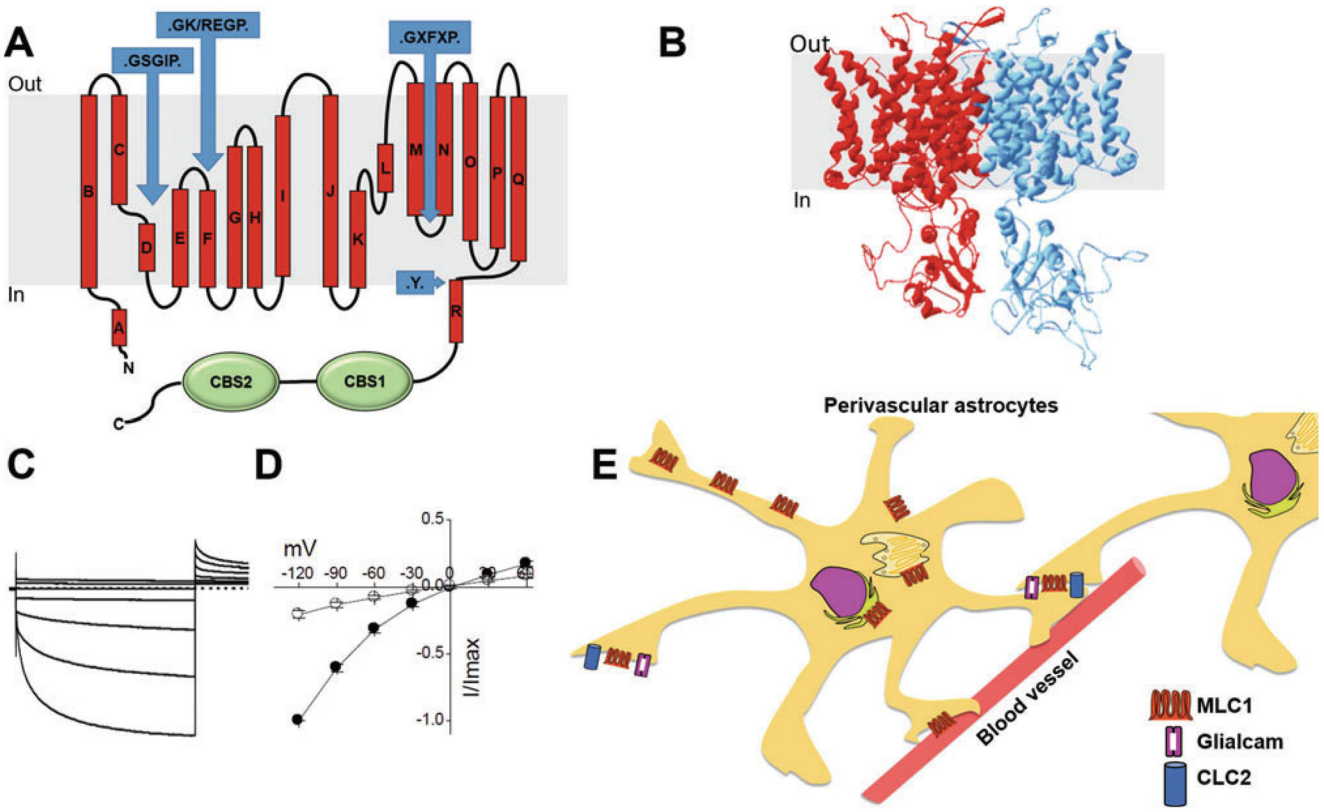

Fig. 10.1.

ClC-2 structure and function. (**a**) Membrane topology of a ClC channel. The 18 α-helices are labeled by letters (A through R). The amino acid sequences that contribute to the Cl^- selectivity are designated by the blue arrows. The two CBS motifs are shown in green. (**b**) Ribbon rendition of rat ClC-2 channel. The two subunits of the dimer are represented in red and blue, respectively. In both A and B, the light gray shaded area represents the plasma membrane. (**c**) Currents elicited by voltage steps from −160 mV to +60 in 20 mV increments from a holding potential of −30 mV in a oocyte expressing rat ClC-2 perfused with a solution in which the main anion was Cl^-. (**d**) Average current/voltage relationship from oocytes injected with rat ClC-2 and perfused with a Cl^- solution (filled circles) and with the Cl^- solution containing 2 mM $CdCl_2$, a ClC-2 channel blocker (empty circles) (n = 8 for both, Sangaletti R., Johnson C.K., and Bianchi L., unpublished observations). (**e**) Perivascular astrocytes showcasing MLC1, Glialcam, and ClC2. All three proteins co-localize to the endfeet of perivascular astrocytes contacting blood vessels and astrocyte–astrocyte contacts [6, 7]. The localization and function of ClC-2 channels are controlled by the interaction with both GlialCAM and MLC1 [8]

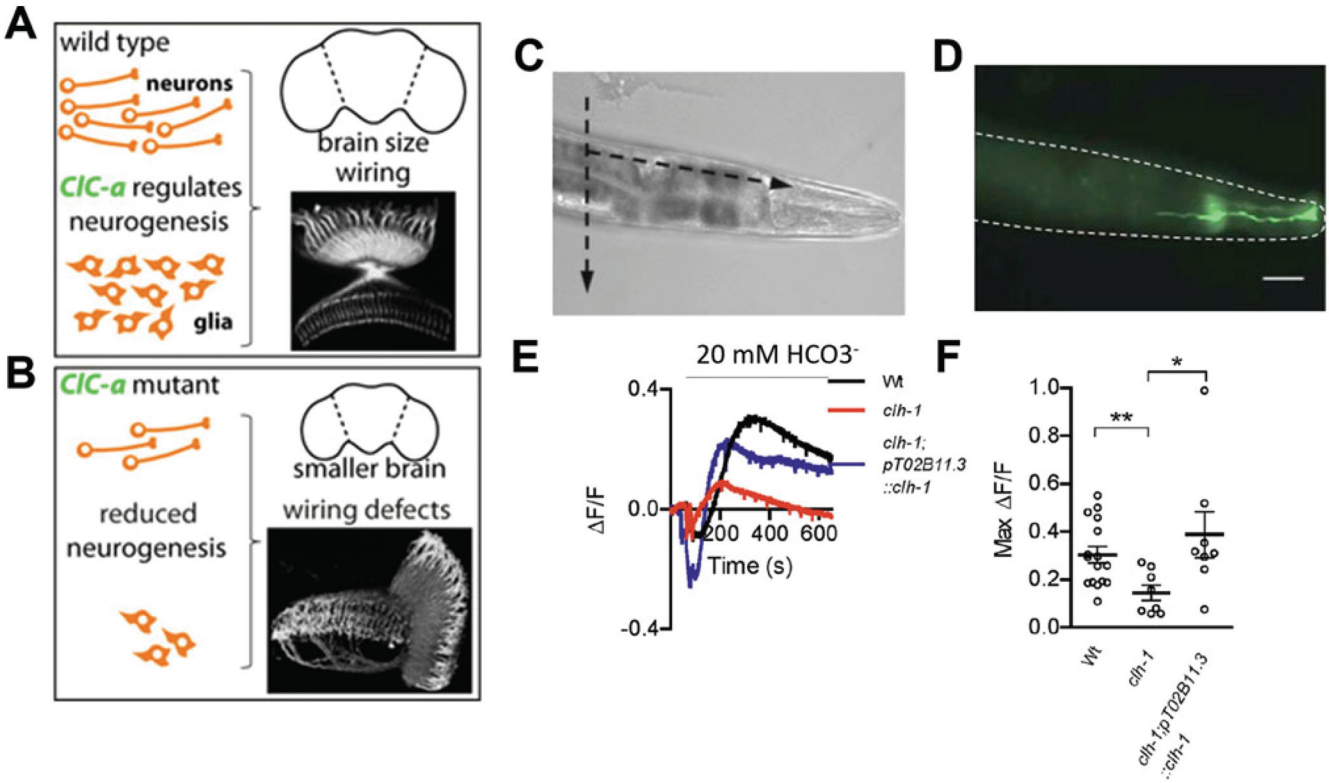

Fig. 10.2.

ClC-2 type channels in Drosophila and *C. elegans*. (**a and b**) In Drosophila, ClC-a is expressed in the niche in cortex glia, which is associated with neurogenic tissues. Analysis of ClC-a mutant flies revealed that ClC-a controls both the wiring of the nervous system and the size of the fly brain. Indeed, in flies that are mutant for ClC-a, the brain is smaller and there are widespread wiring defects. Plazaola and colleagues proposed that ionic homeostasis mediated by glial ClC-a may nonautonomously affect neurogenesis and the assembly of neural circuits [37]. The photographs show representative confocal sections of adult optic lobes of wild type and ClC-a mutant photoreceptor arrays stained with anti-Chaoptin. Apparent is the axonal trajectory defect in the optic lobe of the ClC-a mutant fly. (**c**) Bright-field image of *C. elegans* glued on an agarose pad on a glass slide. The dashed arrows indicate the direction of the cuts made with a glass micropipette prior to pHlourin pH imaging experiments to expose the glia to the perfusing solution. (**d**) Fluorescent image of the same animal as in (**c**). The fluorescence is pHlourin expressed in an amphid sheath glial cell. Scale bars for C and D are 50 μm. (**e**) pHlourin-mediated pH imaging of amphid sheath glial cells in *C. elegans* perfused with an $HCO3^-$ buffer following baseline imaging perfusing with an $HCO3^-$ free and Cl^- free solution. Note the reduced alkalinization in the *clh-1* mutant animal (red line), which is restored in the rescue animal (*clh-1;pT02B11.3:clh-1*, blue line), indicating that CLH-1 is important for $HCO3^-$ permeation into *C. elegans* glia. (**f**) Average alkalinization expressed as DF/F for wild type, *clh-1* mutants, and *clh-1* rescue *C. elegans*, n was 16, 8, and 8 respectively. (**c–f**) were adapted from Grant et al. [38]

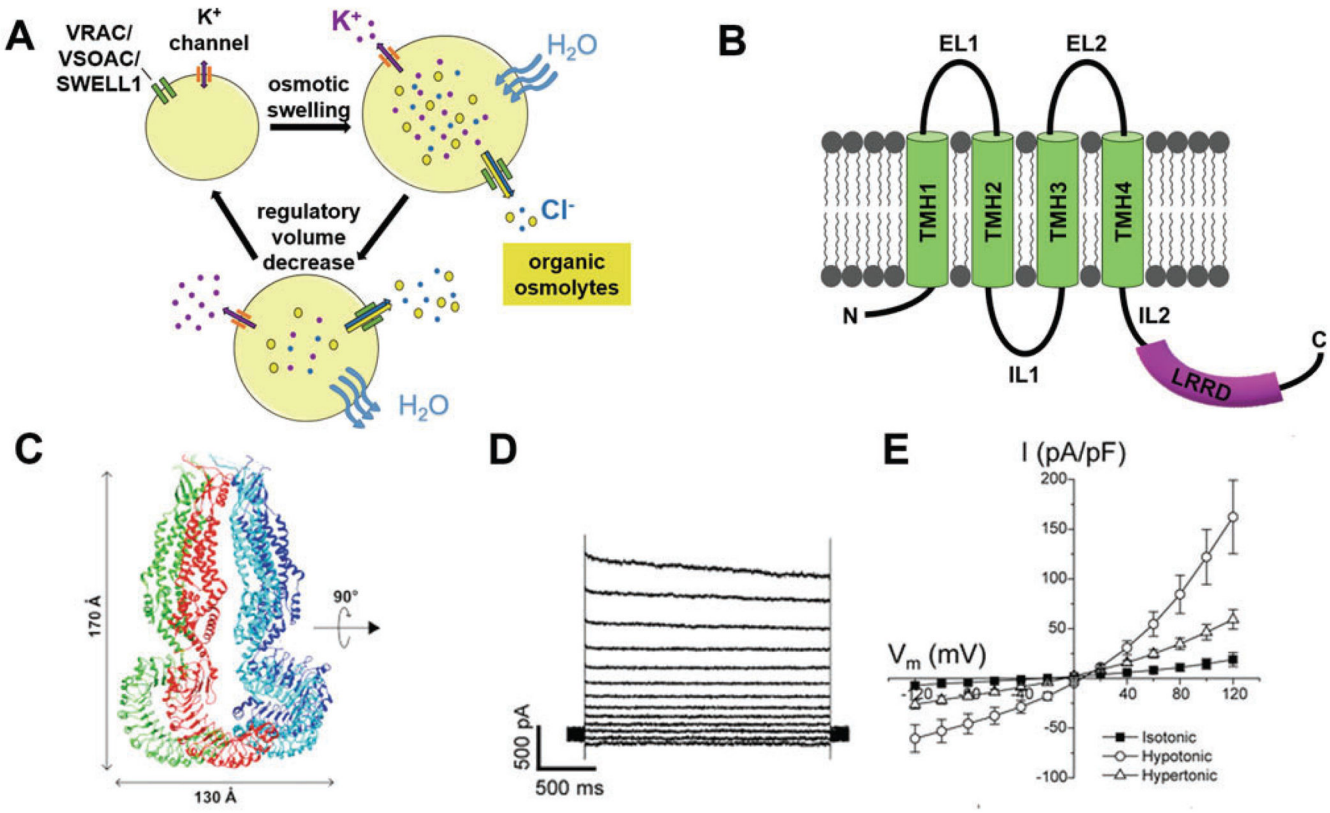

Fig. 10.3.

LRRC8 structure and role in the regulation of volume decrease. (**a**) When cells sense hypotonic conditions they tend to swell causing VRAC/VSOAC/SWELL1 channels to open, allowing for an efflux of organic osmolytes and Cl^-. When the most substrate being transported is Cl^- then VRAC/VSOAC/SWELL1 causes efflux of K^+ via the K^+ channels to maintain electroneutrality. Water efflux across the plasma membrane is induced by the efflux of osmotically active substances. Water efflux is via the lipid bilayer or can be mediated by aquaporins. This mechanism allows the cellular volume to return to its original control level. (**b**) Schematic representation of the topology of an LRRC8 channel subunit. Transmembrane domains are labeled TMH1-4 (Transmembrane Helix 1–4), the extracellular loops are labeled EL1 and EL2 (Extracellular Loop 1 and 2), and the intracellular loops are labeled IL1 and IL2 (Intracellular Loop 1 and 2). The leucine-rich repeat domain (LRRD) is shown in purple. (**c**) Ribbon rendition of LRRC8A hexameric structure. Two subunits in the back are not shown for clarity (from [42]). Each subunit is shown in a different color. (**d**) Example of swelling activated currents in HCT166 cells coexpressing isoforms 8A and 8C of LRRC8. Currents were activated by voltage steps from −120 to +120 mV in 20 mV increments. (**e**) Current–voltage relationships of SWELL1 currents recorded in isotonic, hypertonic, and hypotonic solutions. (**c**, **d**) panels are adapted and reprinted with permission from Yamada and Strange [43]

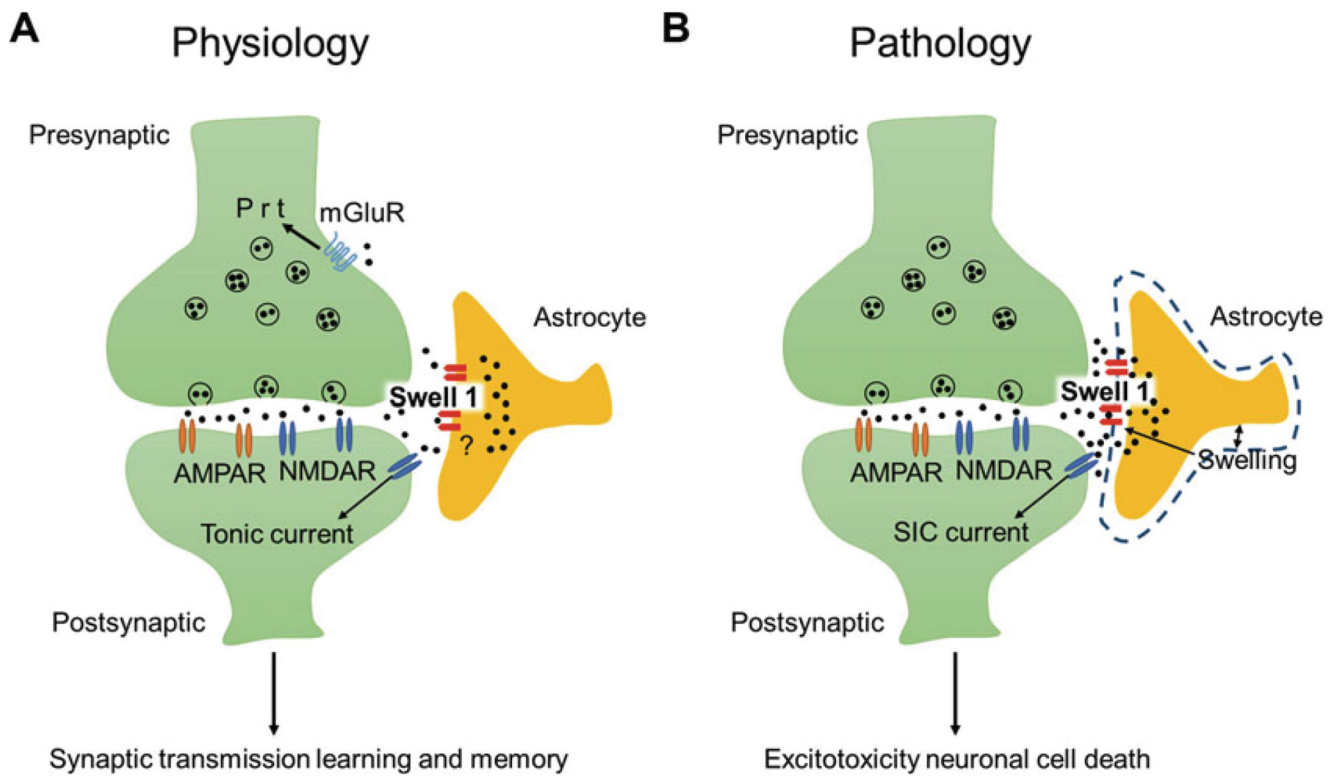

Fig. 10.4.

Role of SWELL1 in learning and memory and in excitotoxicity. Astrocytes contribute to excitotoxicity and regulate synaptic transmission via glutamate release. The exact mechanisms by which astrocytic glutamate is released are not fully understood. VRAC/VSOAC/SWELL1 has been proposed to mediate non-vesicular glutamate release from astrocytes. Indeed, reduced ambient glutamate levels were observed in astrocyte-specific Swell1 knockout mice. These mutant mice exhibited impairment of learning and memory that was dependent on the hippocampus (**a**). Swell1 knockout mice were also protected from brain damage following an ischemic stroke due to reduced glutamate release from astrocytes (**b**) [62]

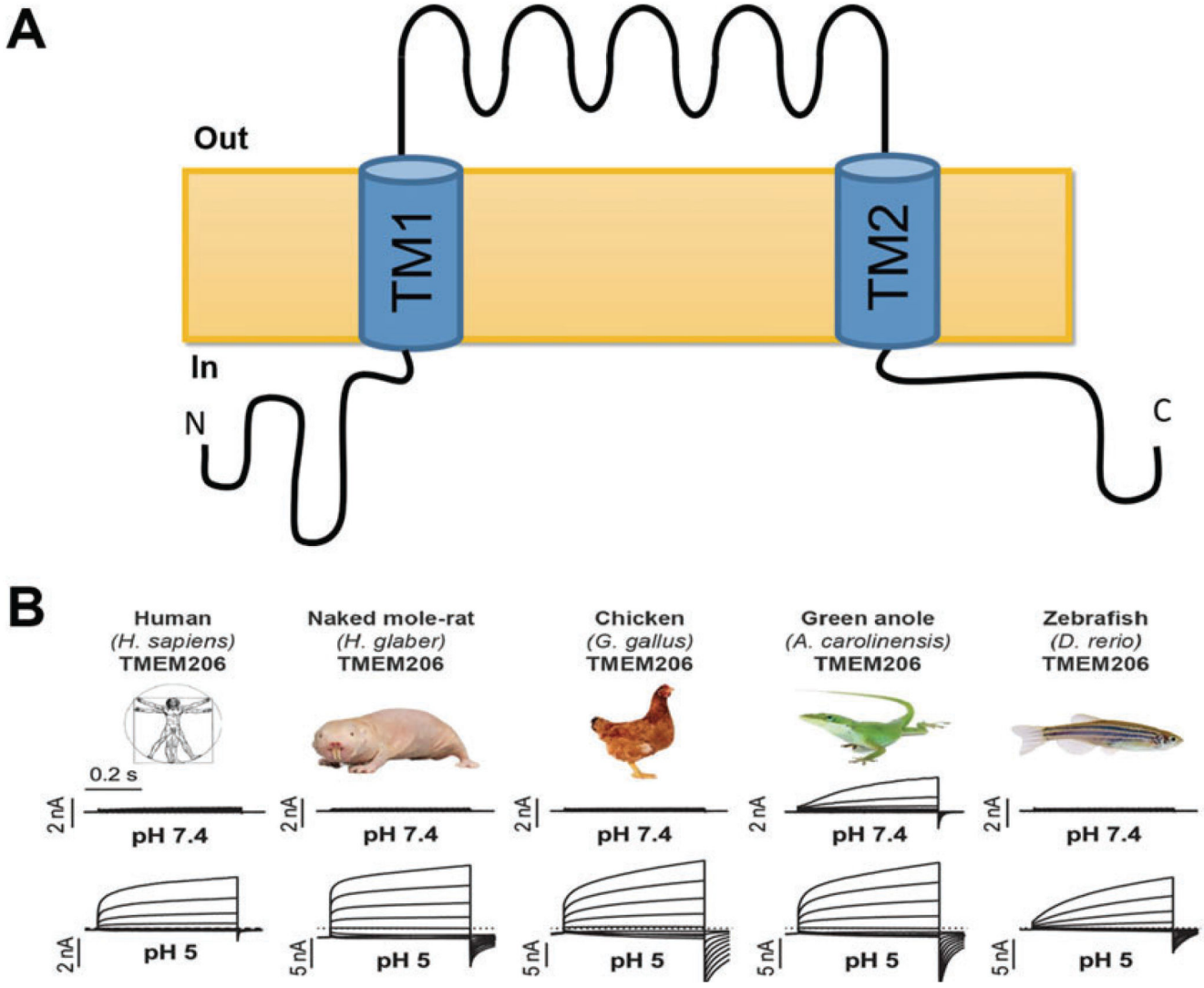

Fig. 10.5.

TMEM206 encodes an acid activated Cl^- channel across species. (**a**) Schematic topology of TMEM206. Human TMEM206 is 411 aa long, it is predicted to have two transmembrane domains (TM1 and TM2) and intracellular N and C termini. (**b**) Human TMEM206 and the corresponding homologs from the naked mole rat, chicken, green anole, and zebrafish expressed in *TMEM206*$^{-/-}$ HEK cells generate Cl^- currents activated by perfusion with a solution at pH 5 [77]

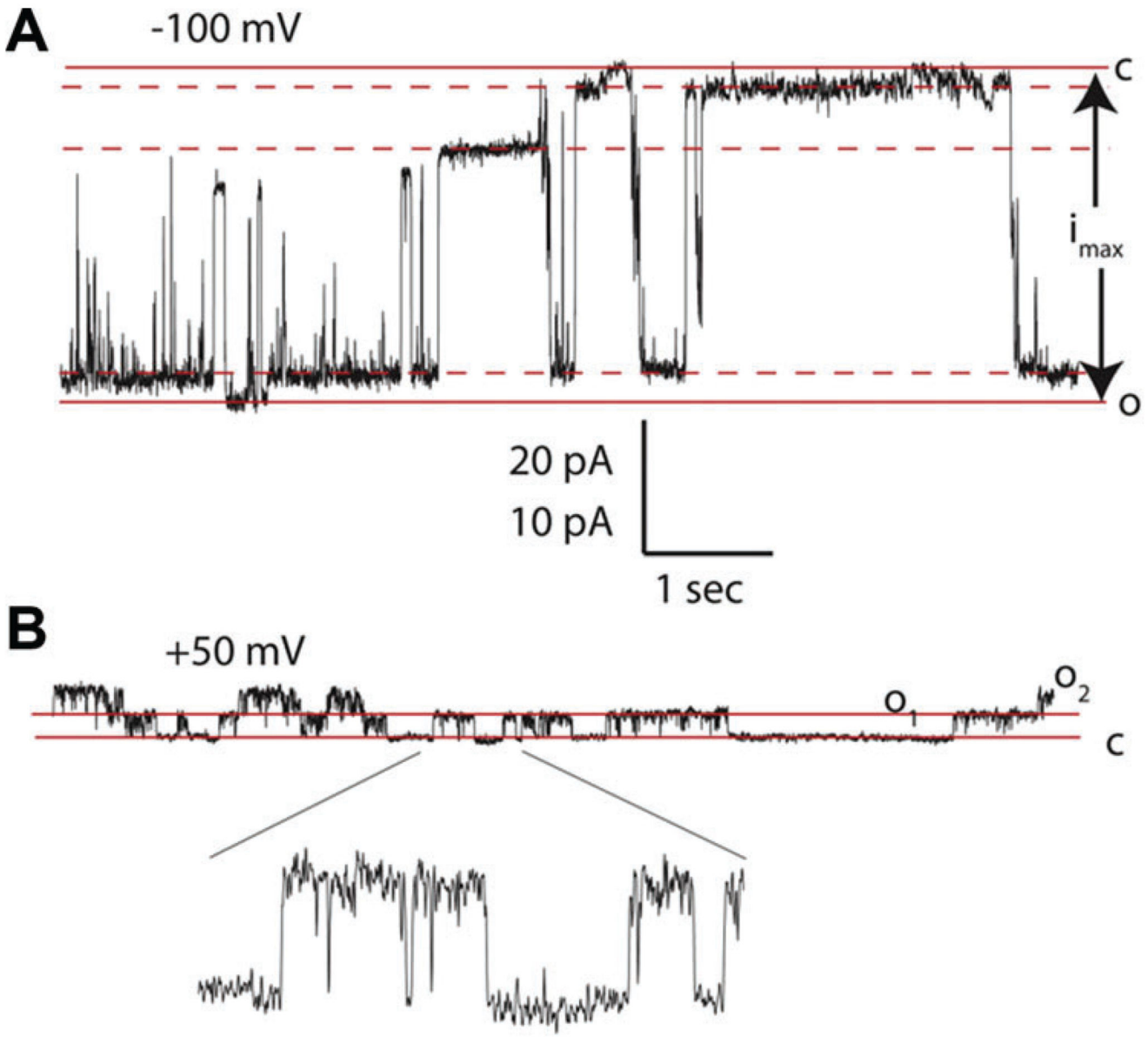

Fig. 10.6.

Pax1 encodes a Cl^- channel when activated by voltage. (**a**) Panx1 opens as a large conductance channel (500 pS) when exposed to high extracellular K^+. The membrane patch was in the inside-out configuration and was clamped at −100 mV. The dashed and solid lines indicate subconductance and fully open and closed states, respectively. (**b**) Panx1 exhibits a low conductance state when activated by voltage. A membrane patch in the outside-out configuration was exposed to low K^+ and clamped at +50 mV. Two small conductance channels, indicated by the red lines and by O1 and O2, are activated under these conditions. One of the channels is also shown on a 5 × scale. The scale shown in panel A applies also to panel B (10 pA). Modified from Wang et al. [107].

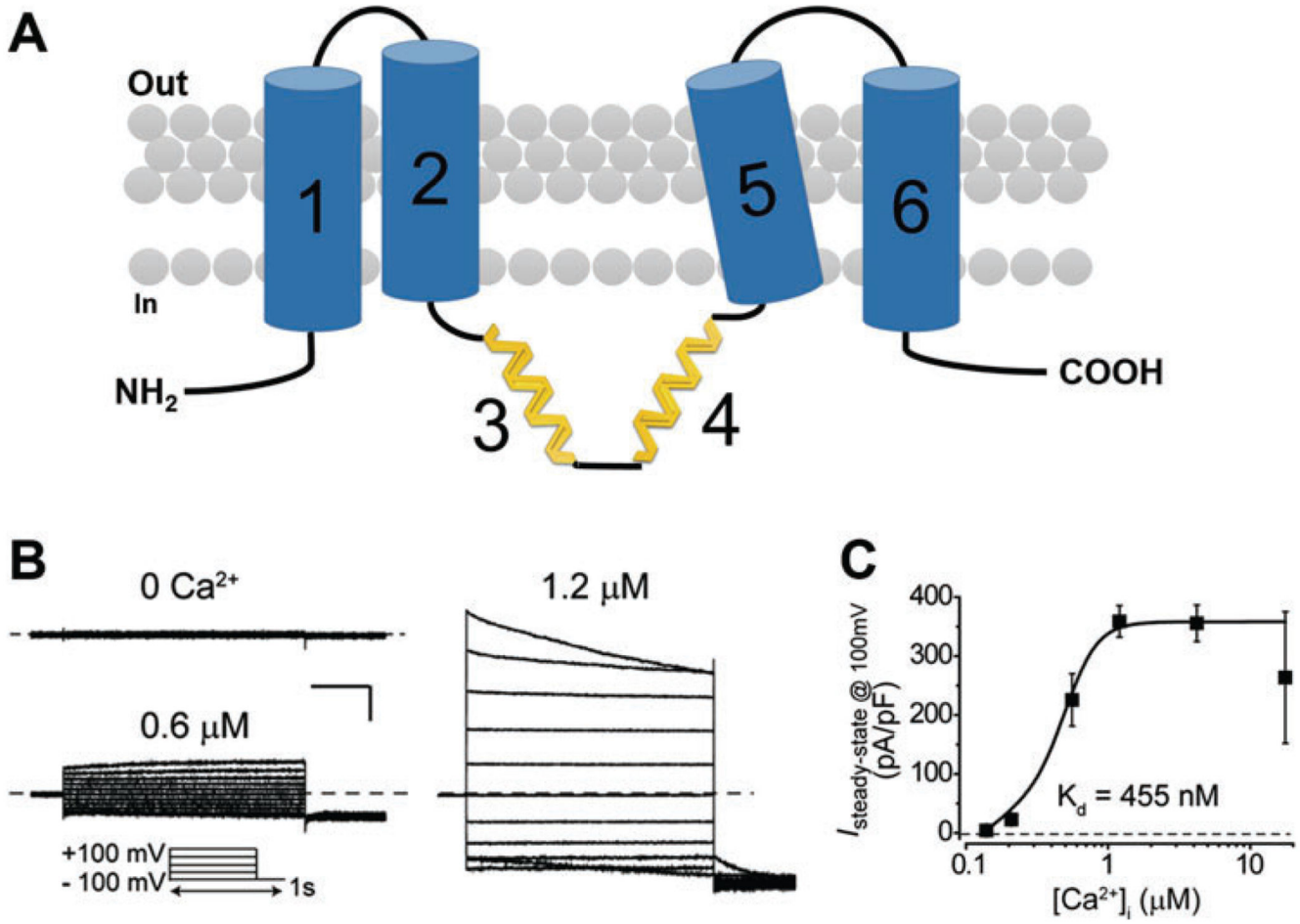

Fig. 10.7.

Bestrophins structure and function. (**a**) Schematic representation of the topology of a Bestrophin channel based on studies conducted on Best1 [132]. There are six hydrophobic domains, however, domains 3 and 4 are expected to be intracellular. (**b**) Best1 currents were recorded in retinal pigment epithelial cells differentiated from induced pluripotent stem cells of a wild-type donor using intracellular solutions containing 0, 0.6 µM, and 1.2 µM Ca^{2+}. The voltage-clamp protocol is shown in the insert. The scale bar is 1 nA and 150 ms. (**c**) Ca^{2+} dose–response curve for Best1 currents similar to the ones shown in panel B. The number of cells tested was 5 or 6 for each data point. The dotted line represents the zero current level. Modified and reprinted with permission from Li et al. [133]

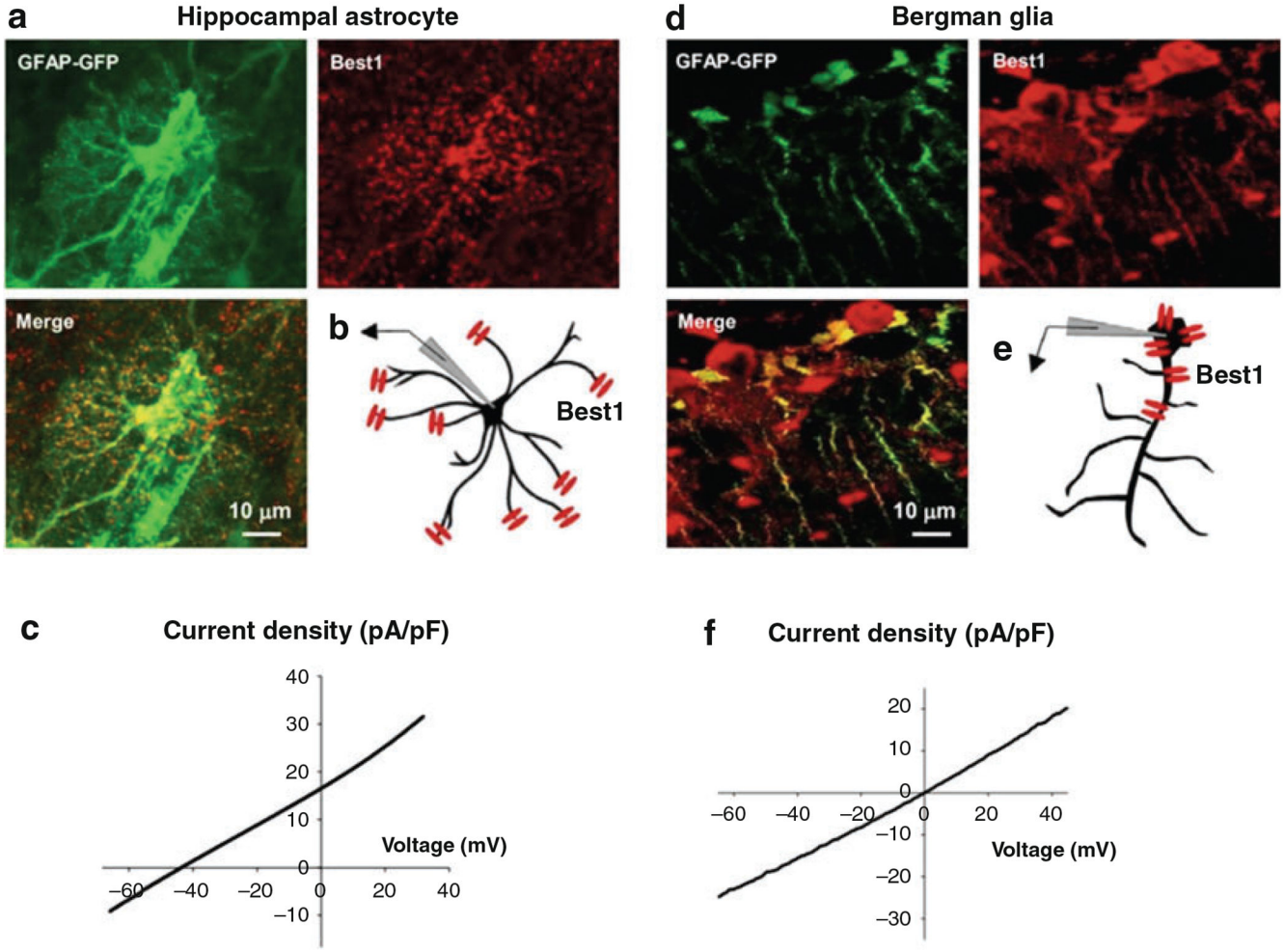

Fig. 10.8.

Best1 localization in hippocampal astrocytes and in Bergman glia. (**a**) Immunohistochemical staining of GFAP-GFP (green) and of Best1(red), and a merge of the two images demonstrating exclusive expression of Best1 channels in microdomains of hippocampal astrocytes. (**b**) Schematic representation of the subcellular localization of Best1 (red) in hippocampal astrocytes. (**c**) Representative current-voltage relationship of NPPB-sensitive currents showing anion conductance in hippocampal astrocytes. (**d**) Immunohistochemical staining of GFAP-GFP (green) and of Best1(red), and a merge of the two images showing exclusive localization of Best1 in the soma of Bergmann glia. (**e**) Schematic representation of the subcellular localization of Best1 in Bergman glia. (**f**) Representative current–voltage relationship of NPPB-sensitive currents in Bergman glia. Note that the experiments shown in **c** and **f** were conducted in isometric Cl^- predicting a reversal potential of 0 mV. The more negative reversal potential observed in hippocampal astrocytes is due to the space clamp error caused by the localization of Best1 at the end of the cellular processes in this cell type. From Park et al. [150]